Scholar Commons
USF University of South Florida

University of South Florida
Scholar Commons

Graduate Theses and Dissertations Graduate School

2007

Effect of temperature on copper chemical mechanical planarization

Veera Raghava R Kakireddy
University of South Florida

Follow this and additional works at: http://scholarcommons.usf.edu/etd

Part of the American Studies Commons

Scholar Commons Citation
Kakireddy, Veera Raghava R, "Effect of temperature on copper chemical mechanical planarization" (2007). *Graduate Theses and Dissertations.*
http://scholarcommons.usf.edu/etd/2236

This Thesis is brought to you for free and open access by the Graduate School at Scholar Commons. It has been accepted for inclusion in Graduate Theses and Dissertations by an authorized administrator of Scholar Commons. For more information, please contact scholarcommons@usf.edu.

Effect of Temperature on Copper Chemical Mechanical Planarization

by

Veera Raghava R. Kakireddy

A thesis submitted in partial fulfillment
of the requirements for the degree of
Master of Science in Electrical Engineering
Department of Electrical Engineering
College of Engineering
University of South Florida

Co-Major Professor: Ashok Kumar, Ph.D.
Co-Major Professor: Shekhar Bhansali, Ph.D.
Wilfrido Moreno, Ph.D.

Date of Approval:
March 28, 2007

Keywords: cof, dishing, defects, pad, metal

© Copyright 2007, Veera Raghava R. Kakireddy

Dedication

I dedicate this work to my beloved parents, family and my friends.

ACKNOWLEDMENTS

I am thankful to everyone who helped me throughout my research work to make this work successful. I thank my family for their love and constant support. I express my deep gratitude and thankfulness to Dr. Ashok Kumar, Major Professor, for providing me with this opportunity to conduct the thesis and also for his guidance and encouragement throughout my research work. I am grateful to Dr. Shekhar Bhansali, Co-major Professor and Dr. Wilfrido Moreno for accepting to be on the committee. I am very thankful to my colleagues and friends in the group, Raghu Mudhivarthi for his valuable suggestions and help during the research work and Sathyaharish Jeedigunta for his support and encouragement. I thank all my friends for their encouragement and moral support during the research period.

Table of Contents

List of Tables iii

List of Figures iv

Abstract vii

Chapter 1 Introduction 1
- 1.1 Multilevel Metallization and I.C's 1
- 1.2 Why CMP 2
- 1.3 Literature Overview 6
- 1.4 Thesis Outline 10

Chapter 2 Understanding CMP 11
- 2.1 The CMP Process 11
- 2.2 Factors Affecting CMP 13
  - 2.2.1 Polishing Pad 13
  - 2.2.2 Slurry 14
  - 2.2.3 Surface Under Polish 16
  - 2.2.4 Pressure 16
  - 2.2.5 Velocity 17
  - 2.2.6 Temperature 17
- 2.3 Copper Significance 18
- 2.4 Copper Deposition Techniques 20
  - 2.4.1 Chemical Vapor Deposition (CVD) 20
  - 2.4.2 Physical Vapor Deposition (PVD) 21
  - 2.4.3 Copper Electroplating 22
  - 2.4.4 Electroless-Plating 23
- 2.5 Copper Removal Mechanism 24
  - 2.5.1 Formation of Surface Layer 25
  - 2.5.2 Abrasion 26
  - 2.5.3 Removal of Abraded Material 26
- 2.6 Pattern Geometry Effects on Removal Mechanism 27
- 2.7 Defects During CMP 27
  - 2.7.1 Dishing 28
  - 2.7.2 Erosion 29
  - 2.7.3 Total Copper/Metal Loss 30
  - 2.7.4 Scratches 30
  - 2.7.5 Wafer to Wafer Non-uniformity 31

2.7.6 Within Wafer Non-uniformity 31
2.8 Summary 31

Chapter 3 Experimental 33
3.1 CMP Testing Tool 33
3.2 CMP Consumables 34
3.3 Experimental Parameters 35
3.4 Estimation of Removal Rate 37
3.5 Post CMP Analysis/Characterization Tools 39
3.5.1 Profilometer 39
3.5.2 Atomic Force Microscopy (AFM) 40
3.5.3 Scanning Electron Microscopy (SEM) 41
3.5.4 Dynamic Mechanical Analysis (DMA) 43
3.5.5 X-Ray Diffraction (XRD) 45
3.6 Summary 47

Chapter 4 Results and Discussion 48
4.1 Dynamic Mechanical Analysis (DMA) of Pads 48
4.2 Scanning Electron Microscopy (SEM) Analysis 50
4.3 Analysis of COF and Removal Rate with Slurry Temperature and Pad 52
4.3.1 Coefficient of Friction (COF) 52
4.3.2 Removal Rate 59
4.4 Analysis of Dishing with Slurry Temperature and Pad 62
4.5 Analysis of Metal Loss with Slurry Temperature and Pad 69
4.6 Analysis of Adhesion Failure and Mechanical Properties with Slurry Temperature 71
4.7 Analysis of Electrical Properties with Slurry Temperature 76
4.8 Summary 80

Chapter 5 Conclusions and Future Work 82
5.1 Conclusions 82
5.1.1 Friction (COF) and Removal Rate Studies 82
5.1.2 Dishing and Metal Loss 83
5.1.3 Film Mechanical and Electrical Properties 85
5.2 Future Work 85

References 87

List of Tables

Table 2.1 Comparison of Properties of Metals 18

Table 3.1 Consumables and Process Parameters for Polishing 35

Table 4.1 Coefficient of Friction at Different Slurry Temperatures Using Slurry-1 57

Table 4.2 Coefficient of Friction at Different Slurry Temperatures Using Slurry-2 58

Table 4.3 Removal Rates at Different Slurry Temperatures Using Slurry 1 and 2 60

Table 4.4 Normalized Dishing Data on Metal Lines and Bond Pads 62

Table 4.5 Mechanical Properties of Copper Thin Films Before and After Polishing 74

List of Figures

Figure 1.1 Cross Section of a Device Showing Various Levels of Metallization	2
Figure 1.2 2005 ITRS – Half Pitch and Gate Length Trends	3
Figure 1.3 Schematic of a CMP Setup	6
Figure 2.1 Schematic of a CVD Process	21
Figure 2.2 Schematic of a PVD Process	22
Figure 2.3 Schematic of a Copper Electroplating System	23
Figure 2.4 Schematic of Copper Removal Mechanism	24
Figure 2.5 Defects Formed During CMP	28
Figure 2.6 Schematic of Copper Dishing During CMP	29
Figure 2.7 Schematic of Erosion Profile	30
Figure 3.1 CMP Bench Top Tester	34
Figure 3.2 Process Flow Diagram for Fabricating the PMOS Devices	37
Figure 3.3 COF vs. Time Graph Used to Estimate Removal Rate	39
Figure 3.4 Schematic of a Profilometer Scan	40
Figure 3.5 Schematic of Operation of an AFM	41
Figure 3.6 SEM Image/Schematic of an AFM Cantilever Tip	41
Figure 3.7 Block Diagram Showing the Operation of a SEM	43
Figure 3.8 DMA 2980 Instrument at USF	45
Figure 3.9 Schematic of an X-Ray Diffractometer	46
Figure 4.1 Storage Modulus and Tan Delta vs. Temperature at 10 Hz Frequency	49

Figure 4.2 Loss Modulus vs. Temperature at 10 Hz Frequency 50

Figure 4.3 SEM Image of Pad A - a) Unconditioned b) Conditioned 51

Figure 4.4 SEM Image of Pad B - a) Unconditioned b) Conditioned 51

Figure 4.5 COF vs. Time of a Sample at 15 °C on Pad A 52

Figure 4.6 COF vs. Time of a Sample at 20 °C on Pad A 53

Figure 4.7 COF vs. Time of a Sample at 25 °C on Pad A 53

Figure 4.8 COF vs. Time of a Sample at 30 °C on Pad A 54

Figure 4.9 COF vs. Time of a Sample at 35 °C on Pad A 54

Figure 4.10 COF vs. Time of a sample at 15 °C on Pad B 55

Figure 4.11 COF vs. Time of a sample at 20 °C on Pad B 55

Figure 4.12 COF vs. Time of a sample at 25 °C on Pad B 56

Figure 4.13 COF vs. Time of a sample at 30 °C on Pad B 56

Figure 4.14 COF vs. Time of a sample at 35 °C on Pad B 57

Figure 4.15 Change in COF vs. Slurry Temperature for Slurry-1 58

Figure 4.16 Change in COF vs. Slurry Temperature for Slurry-2 59

Figure 4.17 Removal Rate vs. Slurry Temperature Using Slurry-1 60

Figure 4.18 Removal Rate vs. Slurry Temperature Using Slurry-2 61

Figure 4.19 Dishing on a 10 µm Wide Metal Line vs. Slurry Temperature Using Slurry-1 63

Figure 4.20 Dishing on a 10 µm Wide Metal Line vs. Slurry Temperature Using Slurry-2 64

Figure 4.21 Dishing on a 20 µm Wide Metal Line vs. Slurry Temperature Using Slurry-1 65

Figure 4.22 Dishing on a 20 µm Wide Metal Line vs. Slurry Temperature Using Slurry-2 65

Figure 4.23 Dishing on a 50 μm Wide Metal Line vs. Slurry Temperature Using Slurry-1 66

Figure 4.24 Dishing on a 50 μm Wide Metal Line vs. Slurry Temperature Using Slurry-2 67

Figure 4.25 Dishing on a 100 μm Bond Pad vs. Slurry Temperature Using Slurry –1 68

Figure 4.26 Dishing on a 100 μm Bond Pad vs. Slurry Temperature Using Slurry –2 68

Figure 4.27 Dishing Profiles of Metal Lines of Different Widths 69

Figure 4.28 Metal Loss vs. Slurry Temperature Using Slurry-1 70

Figure 4.29 Metal Loss vs. Slurry Temperature Using Slurry-2 71

Figure 4.30 Pictures Showing Peeling on Wafers Polished at Different Temperatures 72

Figure 4.31 Graphs Showing XRD Peaks on Copper Wafers Polished at Different Temperatures 73

Figure 4.32 Hardness vs. Displacement into Surface for Unpolished and Polished Copper Samples 75

Figure 4.33 Modulus vs. Displacement into Surface for Polished and Unpolished Copper Samples 75

Figure 4.34 Graphs Showing Transfer Curves (I-V Characteristics) of Wafers Polished at Different Temperatures 77

Figure 4.35 Graphs Showing Sub-Threshold Log Plot Curves (I-V Characteristics) of Wafers Polished at Different Temperature 79

Effect of Temperature on Copper Chemical Mechanical Planarization

Veera Raghava R. Kakireddy

ABSTRACT

The effects of different process parameters on tribology and surface defects were studied till date, but there has been a very minimal study to understand the effect of slurry temperature during Copper Chemical Mechanical Polishing (CMP). The surface defects such as dishing, erosion and metal loss amount for more than 50 % of the defects that hamper the device yield and mainly the electrical properties during the manufacturing process. In this research, the effect of slurry temperature on tribology, surface defects and electrical properties during copper CMP employing different pad materials and slurries has been explored. Experiments were conducted at different slurry temperatures maintaining all the other process parameters constant. Post polished copper samples were analyzed for their dishing and metal loss characteristics. From the results, it was seen that the coefficient of friction and removal rate increased with increase in slurry temperature during polishing with both types of polishing pads. This increase in removal rate is attributed to a combined effect of change in pad mechanical properties and chemical reaction kinetics. The experimental data indicated that the increase in slurry temperature results in an increase in amounts of metal dishing and copper metal loss for one type of slurry and defects decrease with increase in slurry temperature for other type of slurry. This phenomenon indicates the effect of temperature on chemical reaction kinetics and its

influence on defect generation. This can be attributed due to the change in pad asperities due to change in pad mechanical properties and chemical kinetics with change in slurry temperature. The slurry temperature has an effect not only on the surface defects and tribology but also on the change in pad mechanical properties. The copper thin films peeled off at higher polishing temperatures, leading to adhesion failure. With increase in temperature the copper crystallinity, hardness and modulus increased. Further with increase in the defects the electrical properties of the devices also degraded drastically and even failed to operate at higher levels of dishing and metal loss. This research is aimed at understanding the physics governing the defect generation during CMP.

Chapter 1

Introduction

1.1 Multilevel Metallization and I.C's

Shrinking device dimension's associated with ultra large scale integrated circuits is highly effective in achieving high speed performance and in increasing yields at lower cost per chip With the ever increasing thirst to build faster chips the industry is facing the critical problem of integrating the new design rules and also in advancing the Moore's law further. In order to achieve higher circuit density the number of interconnect layers are increased. However when the devices are scaled down the performance falls down as a result for higher circuit density. The higher circuit density causes the devices to slow down due to the increase in interconnect RC time delay of the circuit. As more and more faster devices are built the complexity of fabricating the device with more interconnect layers also increases [1]. In order to assure the performance of the high speed circuits, continuous efforts have been devoted for incorporating copper or low dielectric constant materials into multilevel interconnections for reducing major part of circuit delay, cross talk and power consumption. Till date Aluminum has been the choice of semiconductor manufacturers for the metal contacts, but as aluminum has high resistivity the industry had shifted to copper which has very low resitivity. Also copper has lower electromigration when compared to aluminum. Unlike aluminum, copper cannot be etched and has to be planarized in a different form. Figure.1 shows a typical multilevel metallization circuit consisting of various metallization layers.

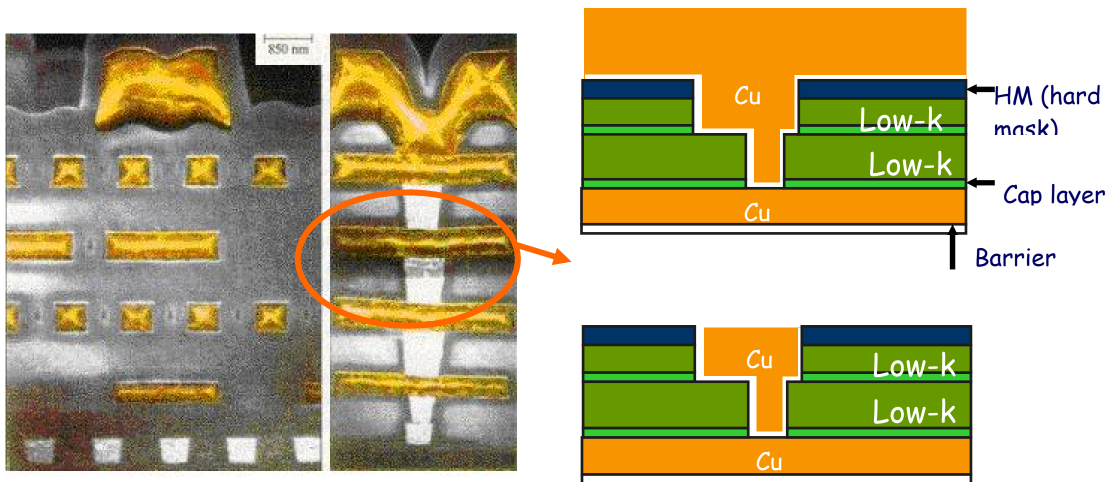

Figure 1.1 Cross Section of a Device Showing Various Levels of Metallization [2]

1.2 Why CMP

With the day-to-day advancement in the field of semiconductor technology and a constant thirst driven by competition for the miniaturization of devices the International Technology Roadmap for Semiconductors (ITRS) which is an association for semiconductor industry has set a goal for achieving various levels of miniaturization in the field of semiconductor industry. Figure.2 shows the levels of metallization and miniaturization set by ITRS. As the number of levels in an interconnect technology is increased, the stacking of additional layers on top of one another produces a more and more rugged topography. The surface of the wafer must be planarized in some fashion to prevent topography roughness from growing with each level. Without such planarization stacking of device features can lead to topography conditions that would eventually reduce the yield of circuits [3].

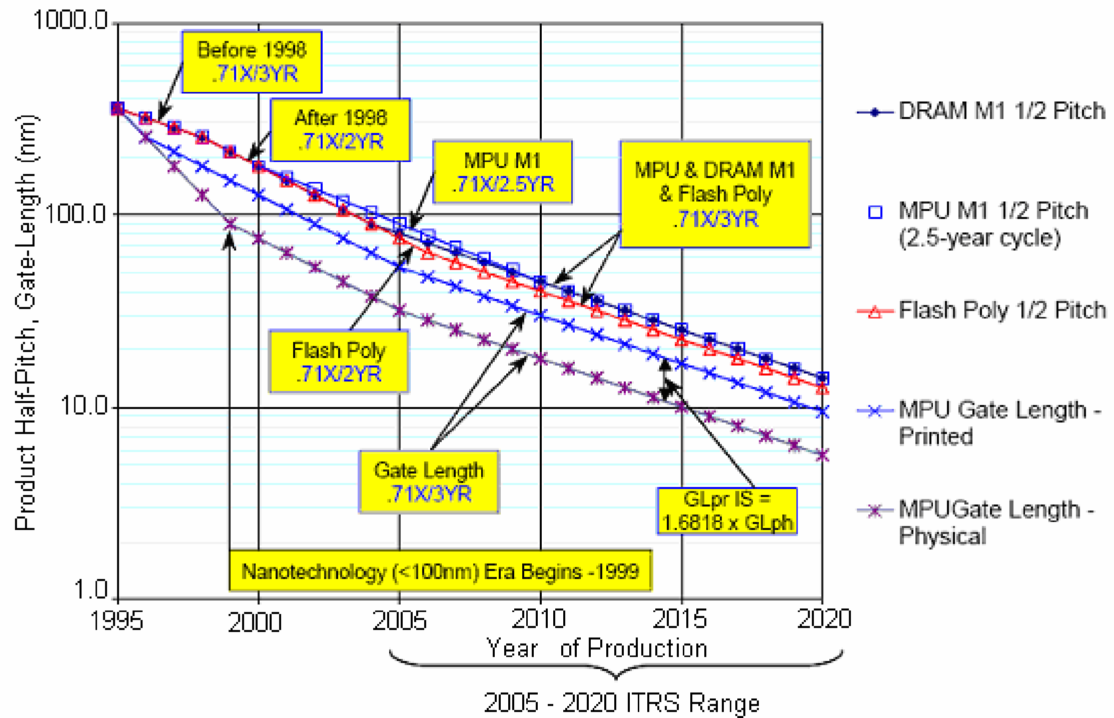

Figure 1.2 2005 ITRS – Half Pitch and Gate Length Trends [4]

Chemical mechanical polishing takes it roots from the glass polishing industry, where it is used to produce ultra smooth finished glass surfaces. Much before the use in semiconductor industry CMP is being used extensively in the glass polishing industry. From just a simple glass polishing technique CMP has been the major process technique to obtain various levels of planarization in semiconductor industry. Chemical Mechanical Planarization (CMP), a process that was pioneered at IBM in the 1980's is the globally used technique to planarize both dielectric and metal layers. With the advancement in semiconductor technology there is a need for global planarization through CMP in order to ensure multilevel copper interconnects. Chemical Mechanical Polishing offers various advantages over other available processes. The advantages of CMP are: [1]

- Universal or materials insensitive - all types of surfaces can be planarized.
- Achieves global planarization.

- Reduces severe topography allowing for fabrication with tighter design rules and multilevel interconnects.
- Provides an alternate means to pattern metal thereby eliminating the need for reactive ion etching or plasma etch for difficult to etch metals and alloys (Eg: Copper).
- Leads to improved metal step coverage.
- Helps in improving reliability, speed and yield of devices.
- Does not use hazardous gases as in the case of dry etching process.
- Low cost process.

The CMP process even with many advantages and desired properties is not without drawbacks such as dishing, erosion etc. Very little has been understood about the effects of temperature during the CMP process. Even though research has been done to study the temperature effect on pad not much has been done to study its affect on surface defects and tribology [5].

Chemical mechanical polishing which is a process of chemical and mechanical action on the surface being processed is dependent on various input process parameters. CMP was initially developed for polishing oxide (SiO_2), which was then used as the interlevel dielectric (ILD) in the multilevel metallization. However with unprecedent advancement in semiconductor technology and introduction of various new dielectric materials, barrier layer materials and copper as metal the CMP development was forced to follow a two fold approach to achieve the required level of planarization of various layers. In this technique, high elevation features are selectively removed resulting in surface with improved planarity [3].

The process of chemical mechanical polishing is performed by mounting the wafer face down on a carrier, which is then forced against a platen with a polishing pad of a polymer such as polyurethane. The carrier and the platen rotate relative motion to each other [3]. A continuous flow of slurry containing abrasive particles is continuously fed onto the surface of polishing pad while the wafer and pad rotate relative to each other. The interaction of both chemical and mechanical effects results in material removal from the wafer surface. The removal rate of the material during CMP is governed by the Preston's equation: [1]

$$\text{Removal Rate (RR)} = K_p * P * V \qquad (1.1)$$

Where P is the pressure applied on the wafer surface, Kp is the Preston's coefficient and V is the linear velocity of the pad relative to the wafer. Preston's equation is the most frequently referenced expression for polishing rates.

Figure 1.3 shows the basic schematic of a CMP setup. The polishing pad usually a polymer is placed on the platen, which rotates a set speed typically in the range of 100 - 200 RPM. The wafer to be planarized is placed on a carrier face down and is pressed down onto the pad surface. The force is applied onto the wafer through the carrier. Proper care has to be taken so that the pressure is uniform at all points on the wafer combined with controlled table motion and carrier rotation rates. The slurry is fed onto the interface of the wafer and pad through a feed pipe at a constant volume. The constant slurry flow allows for uniform planarization and also dissolves the removed material in the slurry from the pad wafer interface. The pads are generally porous in nature and are either grooved or perforated for different applications. The pad is constantly conditioned while

polishing in order to maintain its roughness. The conditioner is usually made of a diamond grid.

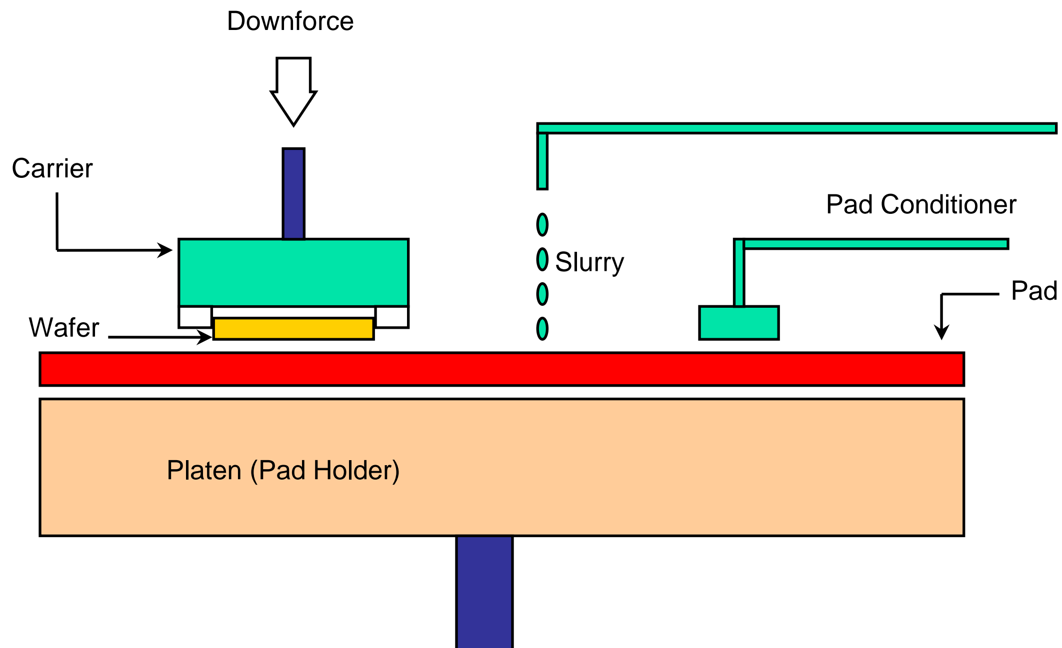

Figure 1.3 Schematic of a CMP Setup

1.3 Literature Overview

With the ever increasing demand for faster performing devices and a constant competition driven industry, till date vast research has been done on various aspects of chemical mechanical polishing (CMP) and still research is being done investigating various aspects of CMP which have been either not looked into or the aspects which couldn't be understood. Various materials are being investigated for use in semiconductor devices. Different low-k dielectric materials have replaced the traditional silicon dioxide (SiO2) which has a dielectric constant ~ 4 with materials of dielectric constant ~ 2.2. Copper has replaced aluminum as the material for contact metal and interconnects. Various reliability studies have been conducted on copper for multilevel metallization

schemes. Chemical mechanical polishing has been the choice of semiconductor industry and researchers for copper removal, as copper cannot be removed by conventional techniques such as wet and dry etching.

Till date research has been done on the CMP of copper looking into various aspects of polishing such as the consumables, process parameters and other input parameters. The chemical mechanisms by which the planarization and removal occur during the chemical mechanical polishing (CMP) of copper have been investigated long back by Steigerwald et al [6]. They proposed that removal occurs as mechanical abrasion of the surface under polish followed by dissolution of abraded particles. Chemical Mechanical Polishing of copper using silica and alumina abrasive particles in different chemistries has been studied by Carpio et al [7]. In their study the problems with formulation of copper slurries were discussed. Slurries with different chemistries have been studied for their reactivity with pad surfaces by Obeng et al [8]. The results showed that the polyurethane pad material is incompatible with some of the chemicals used in CMP, such as hydrogen peroxide. The influence of the slurry chemistry on frictional force in copper during the CMP has been studied by Ishikawa et al [9]. Their study showed that polishing rate increased non-linearly with frictional force, which is controlled by the concentration of slurry chemical constituents.

The effect of slurry surfactant, abrasive size on tribology and kinetics in copper CMP has been determined by Li et al [10]. The abrasive size was a significant factor while surfactant containing formulations showed significant reduction in coefficient of friction (COF). The effects of amount of concentration of abrasive particles were studied by Nomura et al [11] and were found to have a significant affect on the polishing process.

CMP process of two different substrates using copper discs and copper were compared by analyzing their COF's, removal rate and pad temperature analysis by Li et al [12]. Their studies showed that the coefficient of friction and material removal rates were higher for copper deposited wafers. The wear and tear in CMP polyurethane pads due the physical and chemical changes have been analyzed by Lu et al [13]. Their results showed changes in pore geometry of the CMP pads after use due to wear and tear. Properties of CMP polishing pads before and after CMP have been studied using Dynamic Mechanical Analysis (DMA) by Lu et al [14]. The studies showed that mechanical force has shown more significance than chemical action in pad degradation.

The effect of pattern characteristics during copper CMP has been investigated by Wang et al [15]. The copper and ILD CMP have been characterized by looking into some thermal aspects by Sorooshian et al [16]. In their study a modified Preston's equation has been proposed by taking the temperature effect into consideration. A two step copper removal method has been studied for removal of thick copper by Miranda et al [17]. The use of urea and hydrogen peroxide based slurries were investigated by Tsai et al [18]. Their results showed that urea based slurries can achieve better cu CMP. The effects of slurry pH and oxidizer concentration on copper CMP process were studied by Miranda et al [19]. Their study using the design of experiments (DOE) approach showed that the interaction factor of pH and H_2O_2 has dominant effect on CMP process. Delamination during the CMP process in integrating ultra low-k/Cu has been studied by Leduc et al [20].

Chemical Mechanical Polishing of copper in alkaline media such as ammonium hydroxide has been investigated in [21]. Their studies showed that the removal rate

increases with increase in NH_4OH concentration and then at a certain point saturates. Surface generated defects such as pitting corrosion, galvanic corrosion and excessive etching to chemical action has been studied by Miller et al [22]. Their investigation showed that a two step CMP process for Cu/Ta could reduce the defects. Electrochemical characterization of CMP process using hydrogen peroxide as oxidizer and alumina as abrasive particles has been done on copper in [23] and was found that at 1% H_2O_2 concentration the removal rate was maximum and decreased further with increase in H_2O_2 concentration.

The effects of slurry flow rate, pad surface temperature and pad temperature during conditioning on surface tribology and pattern related defects were investigated by Mudhivarthi et al [24]. In their study the pad surface temperature and conditioning temperature were shown to have a significant effect on metal dishing, dielectric erosion and on the nature of conditioning. Their study also indicated that dishing and erosion decreased with increase in slurry flow rate. The increase in amount of dishing was correlated with the increase in pad surface temperature. A study by Mudhivarthi et showed that a change in chemical dissolution rate of copper could be influencing the dishing characteristics [25].

These researches and many others dealt mostly with the fundamental aspects of CMP related to process parameters like pressure, velocity and other consumable characteristics but research based on thermal aspects has not been done extensively. Even though there are some modeling works and a very few experimental works on the effect of temperature on CMP [16, 26, 27, 28], there is a lack of understanding on the effect of

temperature on various aspects of CMP process defects such as dishing, erosion etc. and on tribology during copper CMP.

1.4 Thesis Outline

The aim of this study/thesis is to study the effects of slurry temperature on surface defects such as dishing, dielectric erosion, metal loss and on tribology during copper Chemical Mechanical Polishing (CMP) process. This research is aimed at understanding the physics governing the defect generation during CMP.

The introduction to use of copper, multilevel metallization and use of CMP process to planarize copper, various consumables effecting CMP process and literature overview of copper CMP process has already been discussed in Chapter 1. The Chapter 2 gives a detailed insight about the significance of copper, copper removal mechanism and the available deposition methods for copper. This chapter also gives a detailed overview of various factors effecting CMP process and the consumables used. The CMP polisher used and the experimental setup along with the surface defect generation and effect of slurry temperature on tribology are analyzed in chapter 3. Chapter 4 describes the Post-CMP analysis of polished cu samples using Atomic Force Microscopy (AFM), analysis of pad materials before and after conditioning using Scanning Electron Microscopy (SEM), Dynamic Mechanical Analysis (DMA). Also analysis of polished wafers for device electrical characteristics, due to surface defects and structural changes in copper due to polishing at different temperatures are described. Changes in copper structural characteristics were analyzed using X-ray diffraction (XRD) and nanoindentation studies. Chapter 5 gives an outline about the conclusions from the research work and future work.

Chapter 2

Understanding CMP

Semiconductor industry which is constantly looking for new and better materials to replace the existing interconnect materials in order to reduce the RC delay and size of the device has shifted towards copper as interconnect material from the traditional aluminum. Copper posses several advantages over aluminum and this led the industry to shift towards the use of copper. Copper has properties such as low resistivty and high electromigration resistance required for a good conductor and a interconnect material.

The semiconductor industry shifting towards the use of copper replacing aluminum faced a problem as unlike aluminum, copper cannot be etched and has to be planarized in a different form. Deriving from just a simple glass polishing technique, Chemical Mechanical Planarization (CMP) is the only and most widely used method to planarize copper in the semiconductor industry. Chemical Mechanical Planarization (CMP), a process that was pioneered at IBM is the globally used technique to planarize both dielectric and metal layers.

2.1 The CMP Process

The Chemical Mechanical Polishing (CMP) process was started taking the idea of glass polishing which has been in practice since centuries. Unlike the glass polishing CMP has many more advantages and is a controlled process. The process of CMP was initially used for planarizing oxide, but with the introduction of copper for multilevel

metallization schemes use of Chemical Mechanical Polishing (CMP) has become inevitable. With rapid increase in advancement of semiconductor processing technologies CMP has become a global planarization technique in semiconductor manufacturing.

As said earlier in chapter 1 the process of chemical mechanical polishing is performed by mounting the wafer face down on a carrier, which is then forced against a platen with a polishing pad of a polymer such as polyurethane material. The carrier and the platen rotate relative motion to each other [3]. Slurry containing abrasive particles is constantly fed onto the surface of polishing pad while the wafer and pad rotate relative to each other. The chemical and mechanical interaction then results in material removal from the wafer surface. The removal rate of the material is governed by the Preston's equation [1].

The CMP process which takes place due to the interaction of pad, wafer and slurry form the main consumables and play a significant role. Along with the consumables other factors such as pressure, velocity, temperature, constituents of slurry and various other factors play a considerable role. The significance of each consumable and various factors affecting the Chemical Mechanical Polishing (CMP) process are explained in detail in the flowing sections. The CMP process with many advantages also has some disadvantages such as surface defects (dishing, dielectric erosion, metal loss and erosion), scratches due to particles, pattern dependent non- uniformity, wafer to wafer and within wafer non-uniformity caused due to various process parameters and process consumables.

2.2 Factors Affecting CMP

In a CMP process three main consumables play an important role. Although various other factors such as temperature, pressure and velocity play an important role, the three consumables mentioned below play a major role in a CMP process. They are:

1 Polishing pad.

2 Slurry.

3 Wafer or surface to be polished.

2.2.1 Polishing Pad

Polishing pads are generally made of either a matrix of polyurethane foam with filler material to control hardness or polyurethane impregnated felts. Polyurethane is utilized because urethane chemistry allows the pad characteristics to be varied to meet specific mechanical properties needs. There are various types of polishing pads that are available commercially. Most commonly used pads are the ones that have perforations or groves on the pads. Rodel and Cabot Microelectronics are the two main commercial manufacturers of CMP pads. The polishing pads are porous and pores are introduced intentionally. Pads are made porous as they aid in slurry transport or distribution over the pad surface. Pads used for polishing either have perforations or k-grooves. Researchers and industry are coming out with different kinds of pad materials and pad surface structures. The pad hardness also effects the planarization to great extent. The harder the pads the better is its planarizing ability. Pads with different hardnesses are used for planarizing different materials. The effect of pad hardness along with temperature on planarization process is investigated in this research. To study the pad properties studies such as Dynamic Mechanical Analysis (DMA), Scanning Electron Microscopy (SEM)

and Fourier Transform Infrared Spectroscopy (FTIR) are performed. The DMA explains the change in pad hardness and properties with change in temperature. This helps in understanding the affect of pad on defect generation during CMP with increase in temperature. The SEM images show the pad pore size and wear in pads, as CMP process is a constant wear and tear process due to the friction between surfaces which is a mechanical component. Also the pad degrades due to the chemical effect. Studies by Obeng et al have showed that polyurethane pads are incompatible with chemicals, such as hydrogen peroxide (H_2O_2) [8]. FTIR studies give an understanding about the affect of chemicals on pad.

2.2.2 Slurry

The slurry is one of the main constituent in the chemical mechanical polishing process as the slurry forms the chemical component of the CMP process. The slurry is made up of abrasive particles, oxidizers, buffering agents and complexing agents. Each and every constituent of the slurry plays an important role in polishing process. The principles of electrochemistry are very useful in explaining the chemical mechanisms of metal CMP. The electrochemistry of the slurry explains the process of metal solubility, metal dissolution, and surface layer formation.[1] since CMP is used for a large variety of materials such as oxides, barrier metals and copper, each of these materials has a different chemistry associated with the polishing process. The chemical reaction between the pad and wafer surface modify the mechanical properties of the film, abrasive particles, pad, which in turn affects the mechanical component [1].

The pH of the slurry affects the solubility and dissolution rate of the surface being polished. Various types of buffering agents depending upon the type of slurry are used to maintain the pH constant through out the slurry volume over time. Without the use of which the pH may vary considerably at the wafer surface and in turn may affect the polish rate. In a metal CMP process such as in copper CMP process the chemical reactions are electrochemical in nature. Oxidizers react with the metal surface in order to raise the oxidation state of the metal through a reduction-oxidation reaction, resulting in formation of a surface film on the metal or dissolution of metal. The use of complexing agents increases the solubility of the film being polished. The increase in solubility rate increases the metal removal rate. Hydrogen peroxide (H_2O_2) is the most commonly used oxidizers in a CMP process. The use of various complexing agents such as ammonium hydroxide (NH_4OH) [21], citric acid [29], oxalic acid [30], etc., have been investigated.

The abrasive or the particles used in the slurry provide the necessary mechanical action in a CMP process. The abrasives are made of different materials and are spherical in shape. The diameter of abrasive particles may vary in the range of nanometers to a couple of microns. Silica (SiO_2) particles are the mostly used abrasive particles in oxide CMP, also used in metal CMP such as in copper polishing. Alumina (Al_2O_3) particles are the most commonly used for metal CMP. Other than alumina and silica various other particles such as ceria (CeO_2), magnesium oxide (MgO), titanium dioxide (TiO_2), zirconia (ZrO_2) are used for polishing different materials. The size and hardness of the abrasives also plays an important role as the size of the particle affects the removal rate and surface damage. The abrasive concentration also affects the polishing rate, the material removal rate increases with increase in abrasive concentration.

2.2.3 Surface Under Polish

Wafer or the surface to be polished is also one of the major factors as the feature size, pattern density and material being polished affects the localized pressure distribution which in turn affects the removal rate. The pattern density and feature size thus affect the polishing rate and may cause metal dishing and dielectric erosion. Small features polish quicker than larger features [31]. In planarizing metal over ILD patterned for vias and trenches pattern dependence is observed. The hardness of the wafer surface being polished may also cause scratches or some surface defects. The surface quality affects the yield and also the reliability of the device. The curvature of the wafer also plays a major role in pressure distribution across the wafer surface. This may result in non-uniformity in polishing across the wafer. The stresses in the different film layers may affect planarization, in case of some low-k dielectrics the film might delaminate due to low mechanical strength.

2.2.4 Pressure

Mechanical load or pressure is applied on the wafer surface pressing it downwards during the polishing process. If the surface is rough or has topography, the contact area is less than the geometric area. Due to the topography or rough/uneven surface the pressure is increased until the surface is made smooth. Based on Preston's equation and earlier studies have shown that the material removal rate is proportional to the applied load or pressure [32].

2.2.5 Velocity

The platen velocity plays a significant role in removal rate. The material removal rate is proportional to the pad platen velocity [32]. Slurry transport across the wafer is dependent on the pad velocity. As the pad velocity increases the slurry film thickness decreases and there is an increase in material removal rate.

2.2.6 Temperature

Since the polishing takes place as a result of mechanical interaction of the surface being polished, slurry and the pad, this process in part can be termed as a wear process. Due to the rubbing of two surfaces there is an increase in temperature at the pad – wafer surface interface due to friction. Major part of the temperature increase or heat generated is attributed to the interaction of wafer and slurry interaction and very less due to pad. The increase in the temperature mainly affects the reaction rates. The temperature has considerable effects on the surface defect generation and on tribology during the CMP process. Mudhivarthi et al has investigated the affect of pad conditioning temperature on the removal rate and surface defects [25]. Till date research has been done looking into various aspects such as CMP consumables, pressure, velocity and other factors, but little has been understood about the effect of slurry temperature on the polishing and the tribology. This research aids in understanding the effect of slurry temperature on removal rate, tribology and surface defects such as dishing and erosion during copper CMP.

Also other factors such as thickness, elastic and shear modulus, aging effects of pad, post CMP cleaning, surface quality etc., have a considerable affect on the Chemical

Mechanical Polishing (CMP) process, this research mainly focuses on the effect of slurry temperature and to study the physics governing the copper CMP process.

2.3 Copper Significance

Copper has become the most favorite material in the semiconductor industry for manufacturing the devices. With constant decrease in the size of the semiconductor devices in accordance with the Moore's law the industry search for alternate metal to replace aluminum has resulted with the extensive use of copper as interconnect material. The properties of copper such as good electrical conductivity due to low resistivity of 1.67×10^{-8} Ω-m and high resistance to electromigration has become the ultimate choice of semiconductor industry. The table 2.1 compares various properties of copper with other metals and explains the significance of copper.

Table 2.1 Comparison of Properties of Metals [1]

	Cu	Al	Ag	Au	Al alloy	W
Resistivity (10^{-8} Ω-m)	1.67	2.66	1.59	2.35	3.5	5.65
Electromigration Resistance	Good	Poor	Poor	Very Good	Poor	Very Good
Corrosion Resistance	Fair	Good	Poor	Excellent	Good	Good
Adhesion to Oxide/Low-k	Poor	Good	Poor	Poor	Good	Poor
CVD Processing	Available	None	None	None	None	Available
RIE Etch	None	Available	None	None	Available	Available

From table 2.1 it can be observed that of all the metals listed with low values of resistivity only copper (Cu), silver (Au) and gold (Ag) have low resistivity values compared to aluminum (Al). It could be seen that silver has lower resistivity than that of

copper, but silver diffuses easily into silicon dioxide (SiO_2) and also has poor resistance to electromigration. Whereas copper has good electromigration resistance and search for proper barrier layers to prevent Ag diffusion into oxide couldn't yield any success. Gold (Au) has high resistance to corrosion and electromigration but has higher resistivity compared to copper. Also copper has high melting and boiling points (1357.77, 2835 K) compared to silver (1235, 2435 K) and aluminum (933.5, 2792 K) [33]. Current densities in the lower interconnect levels can lead to electromigration failure. Copper can carry higher current densities compared to aluminum and its alloys and has high electromigration resistance [34].

Copper with all the above properties compared to other available low resistivity metals make it an inevitable choice as a interconnect metal. Even though copper has good properties to be a interconnect metal it has its own drawback and is not without challenges. Copper low adhesion and diffuses easily into oxide/low-k. However researchers have come up with various barrier metals such as tantalum (Ta), tantalum nitride (TaN), titanium (Ti), titanium dioxide (TiO_2) etc., to improve copper adhesion and avoid diffusion into oxide. Copper also is not resistant to corrosion and hence a passivation layer is required. Researchers were successful in finding methods for passivating copper to avoid corrosion [1]. Of all these the major challenge for use of copper as a interconnect metal is copper cannot be etched or patterned using the available wet/dry etch techniques. With the introduction of Chemical Mechanical Polishing (CMP) the problem of patterning copper could be eliminated and copper has found a widespread use in semiconductor industry as a interconnect metal.

2.4 Copper Deposition Techniques

Copper films can be deposited in a number of ways, such as chemical vapor deposition (CVD), physical vapor deposition (PVD), electroplating and electroless plating.

2.4.1 Chemical Vapor Deposition (CVD)

The CVD process uses precursors for copper deposition and organo-mettalic sources are the most commonly used precursors for CVD of copper. Precursors such as copper (II) hexa-fluoro-acetyl-acetonate [$Cu^{II}(hfac)_2$] and $Cu^{I}(hfac)L$, where L is a weakly bonded neutral ligand are used. Copper films of higher quality can be obtained by hydrogen reduction of $Cu^{II}(hfac)_2$. In order to obtain copper films with low resistivity the deposition temperature must be in the range of 350-450 °C, but since use of copper with low-k dielectric materials which are thermally fragile such high deposition temperatures are undesirable. Various deposition process have been developed of which a low-pressure plasma process has been reported which allows for copper deposition at 170 °C and films with comparatively low resistivity can be obtained. Chemical vapor deposition process has issues with depositing void free filling of contact holes and vias. Figure 2.1 shows the schematic of a CVD process.

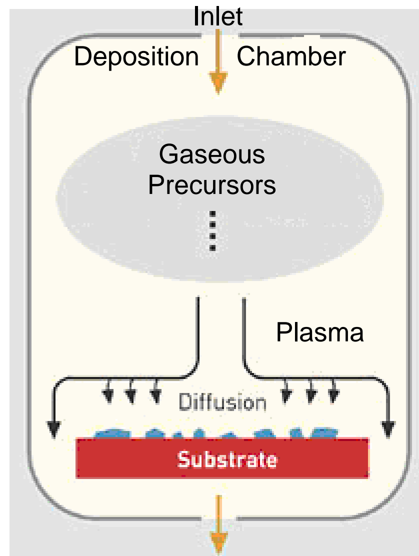

Figure 2.1 Schematic of a CVD Process [35]

2.4.2 Physical Vapor Deposition (PVD)

PVD or sputtering is one of important deposition techniques available to deposit copper. Copper is electroplated for depositing the bulk copper layer. PVD is used to deposit the Cu seed layer which is required to electroplate copper. Sputtering is a physical process whereby atoms in a solid target material are ejected into the gas phase due to bombardment of the material by energetic ions. The impact of an atom or ion on a surface produces sputtering from the surface as a result of the momentum transfer from the in-coming particle. Unlike many other vapor phase techniques there is no melting of the material [33]. Figure 2.2 shows a schematic of a PVD deposition process.

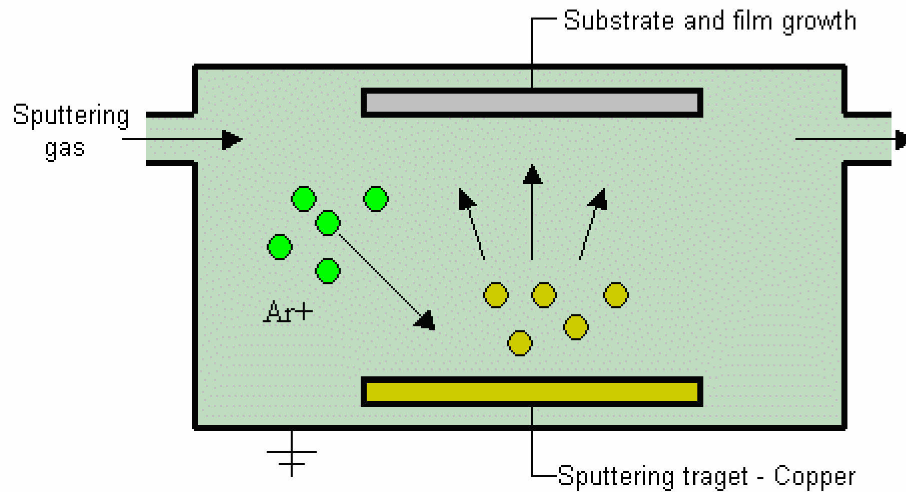

Figure 2.2 Schematic of a PVD Process [33]

2.4.3 Copper Electroplating

Deposition of copper by electroplating technique is the most widely used deposition technique in the semiconductor industry. Since electroplating is a low temperature process it has become the ultimate choice of industry to use it for depositing copper on low-k materials. Electroplating process has high yield output as it has high throughput and also this process can fill high aspect ratio structures. Solutions containing the ions of metal to be deposited are utilized in electroplating process. For copper electroplating a solution containing copper sulfate ($CuSO_4$), sulfuric acid (H_2SO_4), and water is used. The $CuSO_4$ in the solution breaks up into Cu^{2+} and SO_4^{2-} ions. The wafer with a copper seed layer is immersed into the solution and the wafer surface is connected electrically to negative side of an external DC supply source, this acts as a cathode. The positive copper ions are attracted towards the cathode and acquire two electrons and reduces to copper metal, thus depositing (plating) on wafer surface [34, 36]. The reaction that takes place at the cathode is:

$$Cu^{2+} + 2e^{-} \rightarrow Cu \qquad (2.1)$$

The anode is attached to the positive side of the external DC supply source. The rate of electroplating is a direct function of current density. Electroplating process has very high deposition rates. Figure 2.3 shows the schematic of copper electroplating system.

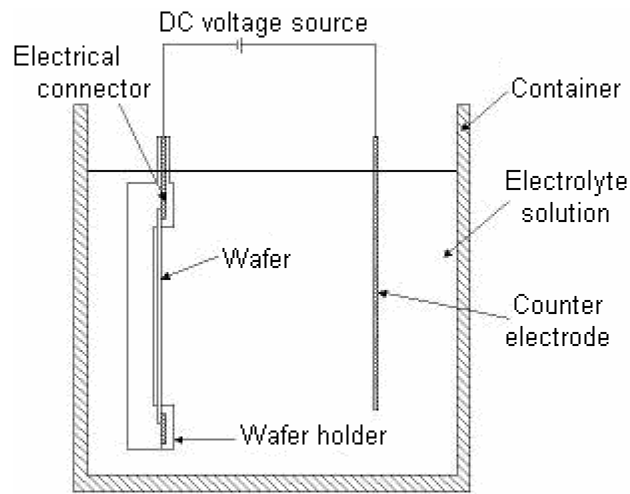

Figure 2.3 Schematic of a Copper Electroplating System [37]

2.4.4 Electroless-Plating

The process of copper deposition through electroless-plating involves the formation of a thin film from an electrolytic solution without externally applied voltage as in case of electroplating. In the electroless process the deposition takes place due to electrochemical reaction between the metal ions, complexing, reducing agent, and pH buffers on catalytic surfaces. The chemical process involves CuO_4 and formaldehyde reduction: [34, 38]

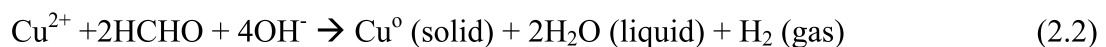

$$Cu^{2+} + 2HCHO + 4OH^{-} \rightarrow Cu^{o}\ (solid) + 2H_2O\ (liquid) + H_2\ (gas) \qquad (2.2)$$

The main challenge in using both electroplating and electroless-plating is to obtain a void free surface.

2.5 Copper Removal Mechanism

Each material has different removal mechanisms as different materials being polished have different hardnesses and removal chemistry. The chemical mechanical polishing (CMP) of copper several differences compared to CMP of oxide/low-k, barrier metals and tungsten. Copper with a hardness of ~ 3 GPa [33] is softer in nature and is easily abraded compared to other materials. The removal of copper basically takes place in about three steps viz., 1) chemical reaction of slurry with copper to form surface layer. 2) Followed by mechanical abrasion of copper surface by abrasives present in slurry. 3) Removal of the abraded copper material from the copper surface. The abraded particles are mostly washed away by the constant flow of slurry onto the pad. Figure 2.4 shows the schematic of copper removal mechanism.

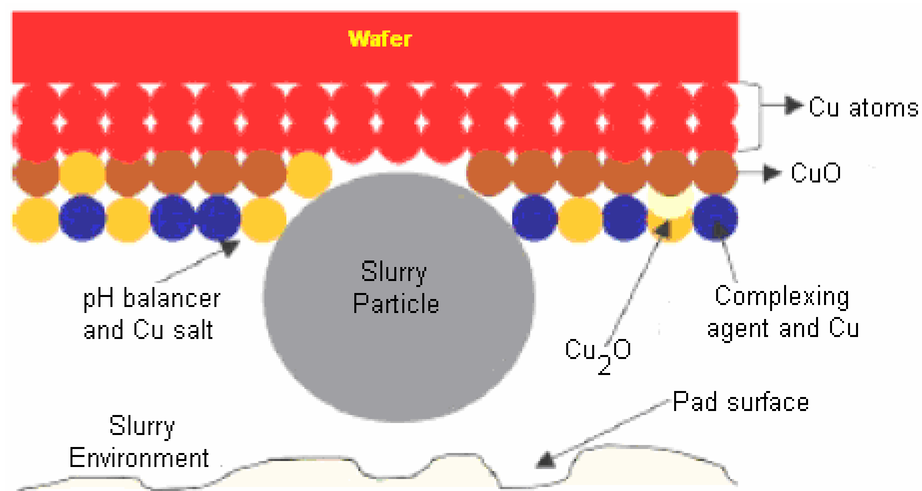

Figure 2.4 Schematic of Copper Removal Mechanism [39]

2.5.1 Formation of Surface Layer

Initially when the wafer surface comes into contact with slurry film it forms a native oxide, hydroxide films, Cu_2O, CuO and $Cu(OH)_2$ surface layer depending upon the slurry being used. Film growth on the surfaces being abraded is controlled by both growth kinetics as well as abrasion dynamics. Copper CMP is generally performed using basic and acidic slurries. Removal rate of copper is low in basic slurries compared to acidic slurries.

Basic slurries usually consist of ammonium hydroxide (NH_4OH), 1 vol% NH_4OH [1]. While using basic slurries a Cu_2O surface layer is formed. The removal rate is low in ammonium hydroxide based slurries. Even though high solubility of copper in ammonia based slurries the low removal rate is due to the formation of Cu_2O layer on the surface. The surface layer acts as a barrier to etching and slows the dissolution of copper.

Acidic slurries usually consist of nitric acid (HNO_3). The acidic slurries generally have low pH values and at low pH values copper doesn't form a surface layer. Studies have shown that as HNO_3 concentration increases the etch rate also increases linearly. This suggests that there no formation of a surface layer. The disadvantage of using acidic slurries is that the high etch rate results in a high removal rate in the recessed areas. The surface is susceptant to corrosion in acidic slurries. In order to avoid corrosion during polishing with acidic slurries a corrosion inhibitor such as benzotriazole (BTA) is added [40]. With addition of BTA a monolayer of Cu-BTA is formed which protects the surface from corrosion.

Due to the corrosive nature of the acidic slurries surface defects such as dishing might take place in the recessed areas. The NH_4OH based does not etch copper and therefore dishing might be only due to the pad reaching into the recessed region.

2.5.2 Abrasion

The abrasive component, whether delivered in a solution phase or abraded form a solid phase, generally provides the mechanical part of CMP. The abrasive particle impacts the surface and abrades the chemically treated surface exposing new material for chemical attack [41]. The particles are either colloidal or non-colloidal in nature. The most commonly used abrasive particles are fumed, colloidal silica, aluminum oxide (Al_2O_3), ceria etc., Copper CMP does not require chemical activity from the particle. In general the size of abrasive particles may vary between 25 nm – 1 micron in diameter.

2.5.3 Removal of Abraded Material

Once the material is abraded from the copper surface the abraded material must be removed from the vicinity of the surface so that it does not redeposit. Since the pad makes constant rotation the chance of the abraded material returning back to surface is high. There have been several ways by which abraded material can be removed. The best method is by passing a constant flow of slurry, due the turbulent motion of the slurry the abraded material is washed away with constant inflow of new slurry. Also different oxidizing agents could be used with basic and acidic slurries so that the copper polish rate may be increased by increasing the dissolution rate of abraded material. This primarily

serves two purposes by increasing the removal rate and by removing the abraded material [1].

2.6 Pattern Geometry Effects on Removal Mechanism

Copper dishing and ILD erosion are the two main undesired defects in CMP process. The dishing and erosion occur during the over polish step which is required to ensure complete copper removal across the entire wafer. The copper dishing can be defined as the difference in height between the center of the copper line, which is the lowest point of the dish, and the point where ILD levels off. Dishing in copper mainly occurs due to bending of polishing pad slightly into the recess to remove the copper from within the recess. Dielectric erosion is a thinning of dielectric layer, resulting because of the reason that the polish rate of oxide is non-zero during the over polish time. The dishing leads to reduction in final thickness of copper line and resulting in complications while adding multiple layers of metal [1] the dishing increases with increase in metal line width.

2.7 Defects During CMP

The chemical mechanical planarization process with many advantages also has some disadvantages in the form of surface defects caused during the planarization process. These defects cause complications while adding multiple layers of metal and other dielectric layers. Figure 2.5 shows some of the defects formed during metal CMP. The various defects formed during CMP are listed below:

1. Dishing
2. Erosion
3. Metal Loss
4. Scratches
5. Wafer to wafer non-uniformity
6. Within wafer non-uniformity

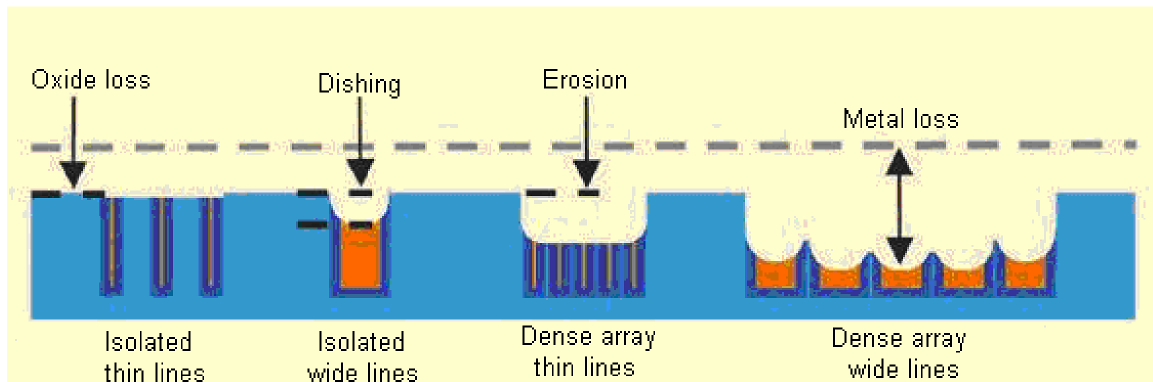

Figure 2.5 Defects Formed During CMP [49]

2.7.1 Dishing

Dishing during copper CMP occurs due to the difference in height between the center of the copper line, which is the lowest point of the dish, and the point where the oxide levels off, which is the highest point of oxide/dielectric. Dishing occurs mainly due to the reason that the pad bends slightly into the recess/interconnect line to remove copper from within the recess. The dishing occurs during the over polish step, which is required to ensure complete copper removal across the wafer. Dishing is undesirable because it reduces the final thickness of the copper line, affects the electrical properties of the device and adds to complexity in adding additional layers of metal. The amount of dishing is dependent or is a function of line width. The dishing also occurs due to nature

of pad physical and mechanical properties. Rigid pads are founds to cause less amount of dishing on patterned wafers. The removal rate of the metal is lower inside the recess because the pad does not exert the same pressure on the recessed surface as on the flat metal surface [1]. The dishing can be reduced by controlling the over polish time closely. Figure 2.6 shows the schematic of copper dishing.

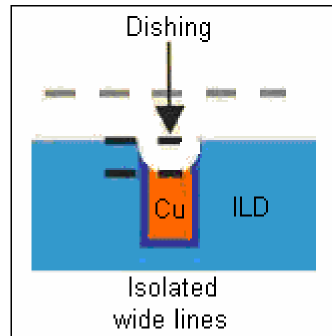

Figure 2.6 Schematic of Copper Dishing During CMP [49]

2.7.2 Erosion

Erosion is the thinning of oxide/dielectric layer caused due to the difference in polish rate between copper and oxide/dielectric during the over polish step. It can be said as the difference in thickness before and after polishing. Oxide erosion is dependent on the pattern density of the features under polish. The removal rate of oxide increases with increase in copper pattern density. This is due to the reason that as the copper pattern density increases there is lesser amount of oxide available to support the force and increase in oxide removal rate. With increase in pattern density tends to cause an increase in pressure on oxide thus increasing the oxide polish rate. Erosion during polishing is undesirable as it degrades the electrical properties of the device and increases the process complexity while adding more layers over it and finally may short the device electrically.

The oxide erosion can be reduced or avoided by reducing the copper over polish time [1]. Figure 2.7 shows the schematic of an interlayer dielectric (ILD) erosion profile.

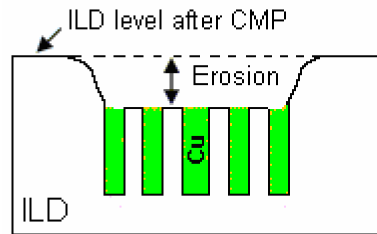

Figure 2.7 Schematic of Erosion Profile

2.7.3 Total Copper/Metal Loss

The total copper loss or metal loss is the loss or removal of metal in the patterns of higher copper widths. The copper loss occurs due to difference in removal rates between the adjacent materials and also due to pattern dependency. This causes to affect the device operating characteristics and is undesirable in a CMP process.

2.7.4 Scratches

Scratches during polishing mainly occur due to the abrasive particles used. Since copper is softer in nature the abrasive particle due to their properties and mechanical properties may cause scratches on the copper surface. The scratch can be identified by the depth and no of the scratches caused by the abrasive particles. In order to avoid scratches abrasive particles softer in nature may be used. Scratches may have an affect on the overlying layers during processing and next step of polishing.

2.7.5 Wafer to Wafer Non-uniformity

Wafer to wafer non-uniformity (WTWNU) is the difference in the amount of the polishing observed between wafer to wafer. This may be caused due to various process parameters controllable and uncontrollable. The WTWNU is caused due to decay in material removal rate with polishing more number of wafers on the same pad for a longer time [50]. This may also due to the change in wafer surface properties.

2.7.6 Within Wafer Non-uniformity

The within wafer non-uniformity (WIWNU) is due to the variation in material removal rate in CMP process. It has been observed that even with a uniform down force the material removal rate is not uniform across the wafer [50]. The non-uniformity in polishing may be caused due to degrading pad polishing properties or may be due to non-uniformity in the applied down force across the wafer surface.

2.8 Summary

With shrinking device dimensions and increasing RC delay there has been an extensive search for various new metals to replace aluminum as a interconnect material. Various materials as potential replacements were considered but copper a good electrical conductor with low resistivity, high current density and high electromigration resistance has replaced aluminum as the interconnect material. Although copper possesses all the characteristics of a good electrical conductor it also has some disadvantages or complications. Unlike aluminum copper cannot be etched, which was overcomed by introduction of Chemical Mechanical Polishing (CMP) where copper is etched due to

interaction of chemical and mechanical components. First the surface is altered chemically and then abraded away by the abrasive particles present in the slurry. Copper also diffuses easily into oxide/low-k dielectrics and in order to avoid this barrier layer has to be deposited. Copper can be deposited by various methods, such as CVD, PVD, electroplating and electroless-plating. Copper with all characteristics of a good electrical conductor has assumed a significant place in semiconductor manufacturing as an interconnect material. Copper CMP with its advantages also has some problems that are caused due to surface defects such as dishing, erosion, scratches, wafer to wafer non-uniformity and within wafer non-uniformity. These defects can be minimized by reducing the over polish time and by selectively choosing the polishing pads and other consumables.

Chapter 3

Experimental

3.1 CMP Testing Tool

The experimental work for this research work has been carried on a CETR CP-2 CMP bench top polisher provided by CETR Inc., USA. The CMP process on this bench top polisher closely imitates large wafer fabrication production processes. The CMP tester generates real time lateral and normal force data. These signals can be monitored and analyzed in-situ. Figure 3.1 shows the picture of the CMP bench top polisher used at University of South Florida.

The bench top tester has an upper and lower platen which can rotate at speeds from 0.001-5000 rpm. The lower platen is used to hold a polishing pad of 6” in diameter. The upper platen can hold a wafer upto 2” in diameter. The upper platen is connected to a vertical linear motor that has a travel length upto 150 mm. the tester has ultra accurate strain-gauge sensors which can measure the load (0-10 Kg) and torque in two to six axes. The forces can be measured with a resolution of 0.1% and precisely in the range of milligrams to kilograms with very high repeatability. The upper platen is positioned on a slider assembly, which can slide in the X-Y direction. The tester has a fully automated PC based interface for motor control and data acquisition.

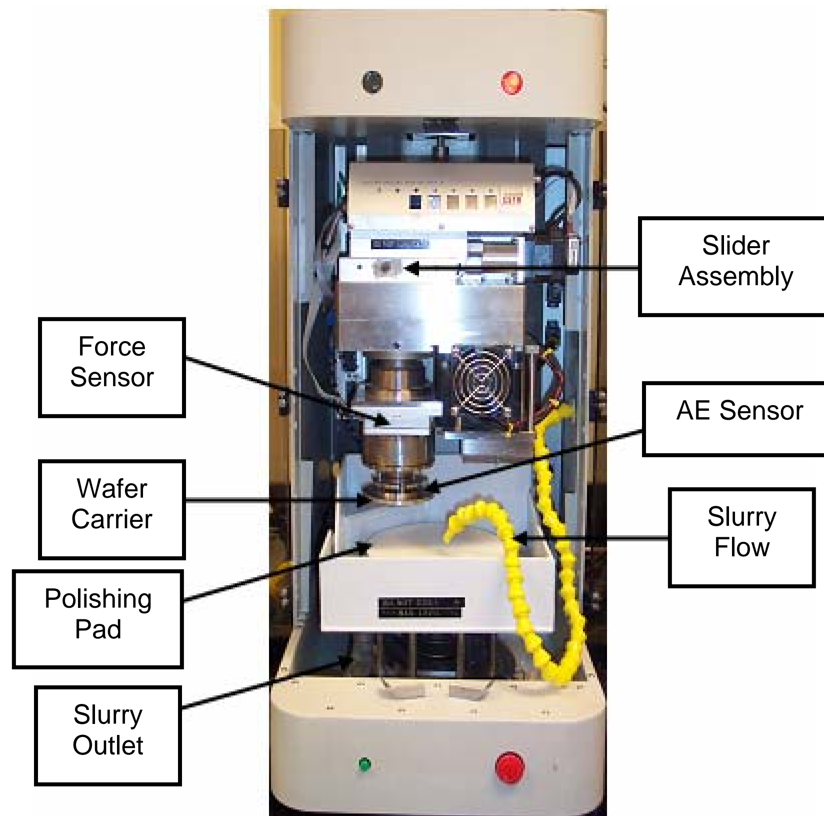

Figure 3.1 CMP Bench Top Tester

3.2 CMP Consumables

The experiments were carried out on 2 cm X 2 cm patterned copper wafers having MIT 854 structure. The patterned copper samples had a barrier and low-k layers beneath the copper. The samples were polished using two different kinds of polishing pad and copper slurry containing colloidal silica as abrasive particles. The polishing pads used were Pad A with SUBA IV subpad and Pad B. Subpads were used with both the polishing pads in order to reduce the non-uniformity during polishing. Hydrogen peroxide (H_2O_2) was used as the oxidizer in the slurry for polishing. The pad was conditioned using deionized (DI) water for 10 minutes prior to polishing each sample to

increase the roughness of the pad. The initial thickness of copper on the unpolished samples was 1 μm.

3.3 Experimental Parameters

The consumables and the process parameters used for the polishing experiments are listed in table 3.1.

Table 3.1 Consumables and Process Parameters for Polishing

Parameters and Consumables	Description
1. Polishing Pressure	3 psi
2. Velocity	150 rpm (0.5 m/sec)
3. Slider Motion	5 mm offset at a speed of 1 mm
4. Pad Conditioning Pressure	1 psi
5. Slurry Flow Rate	75 mL/min
6. Polishing Pad	Two types of pads with k-grooves
7. Slurry	Three types of commercial copper slurry (Two for first two series of experiments & other one for the third series of experiments)
8. Oxidizer	Hydrogen Peroxide (for two types of slurries) and APS for third slurry.
9. Slurry Temperature	15, 20, 25, 30 and 35 °C
10. Wafer/Sample	2 inch wafers with 10000 A° copper over patterned low-k dielectric for dishing experiments with MIT 854 structure for dishing and metal loss experiments 3 inch wafers with 10000 A° copper over patterned silicon dioxide for determination of device electrical properties 2 inch blanket copper wafers with 10000 A° copper for determination of any structural changes

The patterned copper samples were 2 inch wafers with MIT 854 structure and were polished using two different pads, pad A and pad B with subpads. The pad A has perforations in it and pad B polishing pad has k-grooves in it. Pad B is softer in nature compared to pad A. The pads were conditioned for 10 minutes prior to polishing each sample to ensure that the pad roughness remained constant throughout the polishing process. The pressure and platen velocity were maintained constantly at 3psi and 150 rpm through out the polishing. The slider was allowed to oscillate 5mm in X-Y direction at a velocity of 1mm/sec. The slurry temperature was varied at 15 °C, 20 °C, 25 °C, 30 °C and 35 °C. The slurry temperature was controlled for each experiment during the whole project by monitoring and maintaining the temperature at a specific value within a 0.2 ^{o}C variation using a temperature controller.

Temperatures below and above room temperature were investigated as there is a very minimal probability of slurry temperature going down very low or very high; also as heat is generated during polishing to rubbing of two surfaces there is a raise in temperature. As recommended by the manufacturer the temperatures above 40 °C were avoided as the slurry would undergo changes chemically and would be rendered useless. Hydrogen peroxide (H_2O_2) was added to the slurry as an oxidizer. Figure 3.2 shows the process steps for the PMOS device fabricated for testing the electrical properties. The wafers used were 3 inch, type <100> orientation and N-type silicon wafers. In order to make it a P-type device it was doped with a P-type (boron) spin on dopant. The process was a three mask process, used for defining the diffusion areas, gate and regions for the metal interconnects. A thin layer of Tantalum of 25 nm thickness was used as a barrier and adhesion layer for copper. A 1 μm thick copper layer was deposited using

electroplating method. The wafers were than polished and tested for the electrical properties.

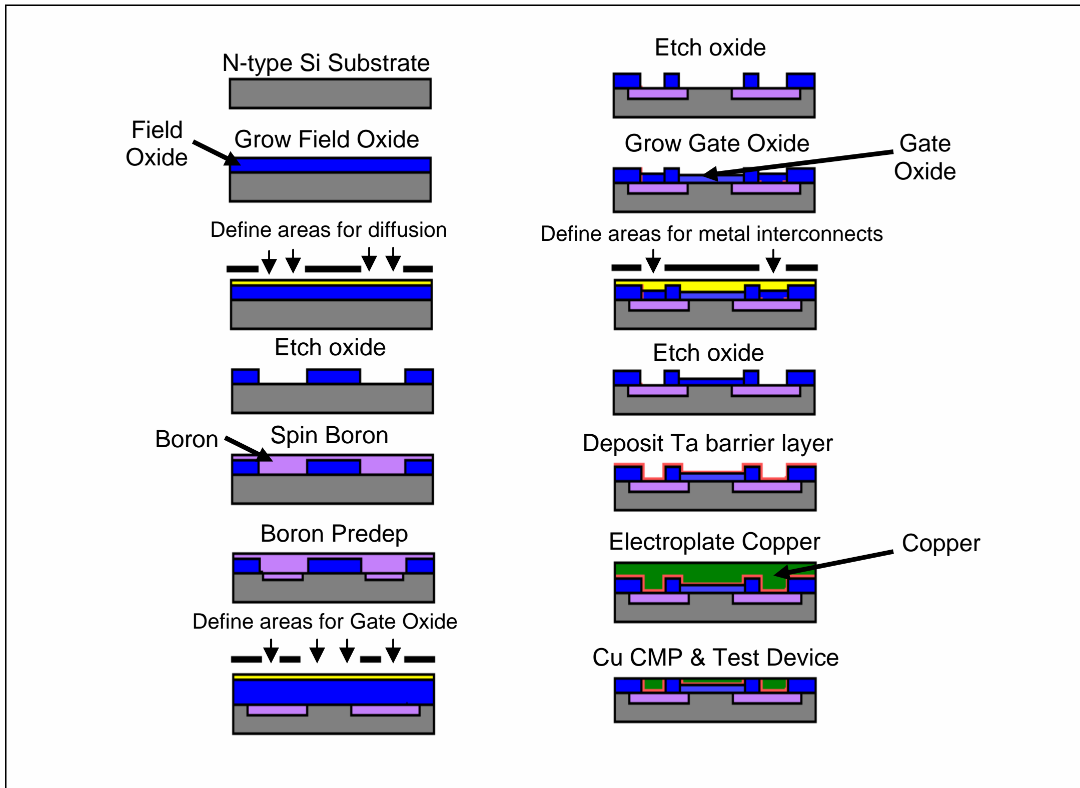

Figure 3.2 Process Flow Diagram for Fabricating the PMOS Devices

3.4 Estimation of Removal Rate

During the polishing the coefficient of friction (COF) is continuously monitored in-situ at a sampling rate of 20 kHz and recorded. The COF at the pad-wafer interface, which changes between the wafer layers (metal, barrier and oxide) in contact with pad, indicates the material removal time and allows for calculation of material removal rate [52,53], friction force and coefficient in the wafer–pad interface, changes which allow for precise detection of the start-point and end-point of removal; [54] pad wear, temperature of the slurry and/or on the pad; and contact acoustic emission in the wafer–pad interface,

the average level of which allows for evaluation of polishing intensity and peaks allow for detection of wafer scratching and layer delamination processes. [52]

The in situ monitoring of the coefficient of friction between the wafer and the pad provides understanding of the tribological mechanisms occurring at the interface and also facilitates precise end-point detection of the polishing process. This method of end-point detection overcomes challenges posed by other methods like normal reflection, eddy current systems, etc. These other methods are applicable only to a limited set of material types used depending on the material optical and electrical properties. As the coefficient of friction is specific to the material type and the characteristics of the interface, it changes as soon as the material type at the interface changes upon the initial exposure of the underlying film. Thus, in situ monitoring of the coefficient of friction during CMP provides precise end-point detection irrespective of the optical and electrical properties of the material being polished.

The in situ monitoring of the coefficient of friction between the conditioner and the pad facilitates precise detection of start and end points of polishing and allows for optimization of the material removal process.[54] The details and capabilities of the instrument are discussed elsewhere extensively. [52, 55, 56] Figure 3.3 shows the graph of COF vs. time used to estimate the removal rate.

The removal rate (RR) in nm/min (units) was calculated as follows (3.1):

$$\text{Removal Rate (RR)} = \text{Thickness of Copper} / \text{Time taken to remove whole copper} \quad (3.1)$$

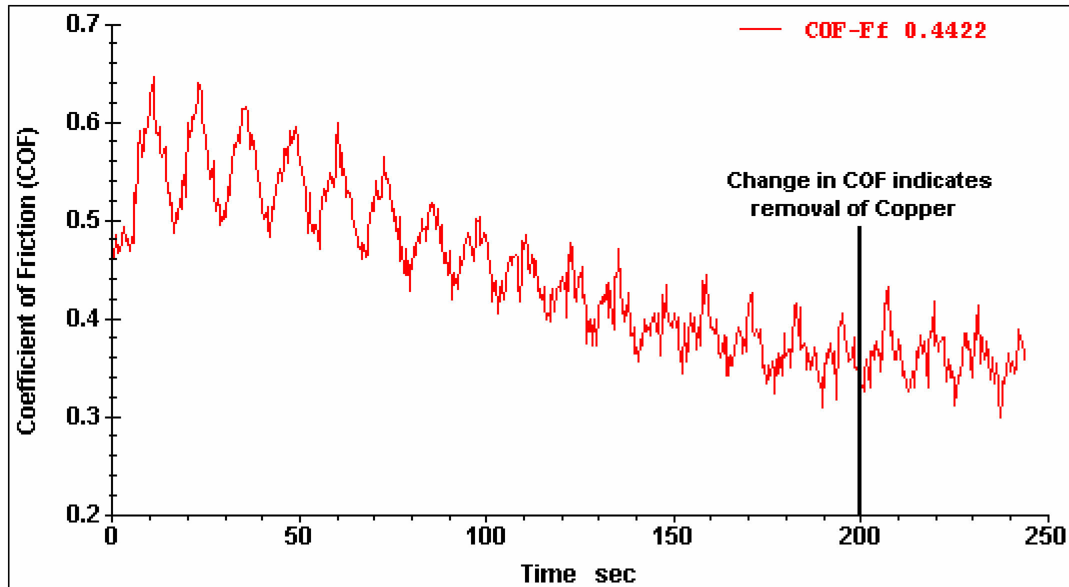

Figure 3.3 COF vs. Time Graph Used to Estimate Removal Rate

Initially at each temperature a sample was polished for total removal and using the change in COF the removal rate was calculated. Using the calculated time for removal the experimental patterned copper samples were polished for removal rate, COF, dishing and erosion values with a 10% over polishing time to ensure that the copper is completely removed.

3.5 Post CMP Analysis/Characterization Tools

3.5.1 Profilometer

The Profilometer uses a diamond tip to scan a surface to get information about surface topography. Like any scanning probe, the tip has a finite surface area which interacts with the sample being scanned. Figure 3.4 shows the schematic of operation of a profilometer.

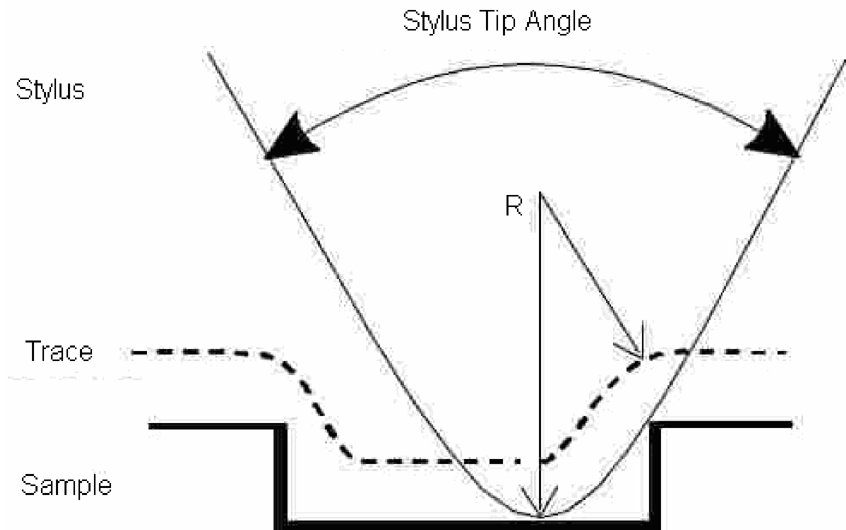

Figure 3.4 Schematic of a Profilometer Scan

The tip scans across the surface of the sample, and an inductive sensor registers the vertical motion of the tip. The signal generated by the motion of the tip is used to create a two-dimensional profile of the surface from which the step height can be calculated [42].

3.5.2 Atomic Force Microscopy (AFM)

The atomic force microscopy (AFM) works similar to the same way as a profilometer works, only on a much, much smaller scale. The AFM consists of a microscale cantilever with a sharp tip (probe) at its end that is used to scan the specimen surface. The cantilever is typically made of silicon or silicon nitride with a tip radius of curvature on the order of about 10 nanometers. When the tip is brought into proximity of a sample surface, forces between the tip and the sample lead to a deflection of the cantilever according to Hooke's law. The change in the vertical position (due to repulsive or attractive Van der Waals force) reflects the topography of the surface. By collecting the height data for a succession of lines it is possible to form a three dimensional map of

the surface features. A tip or cantilever which drags across the surface of the sample is specially constructed for surface structure investigation. Figure 3.5 shows the schematic of an AFM and figure 3.6 shows the SEM picture/schematic of an AFM cantilever/tip [33, 42].

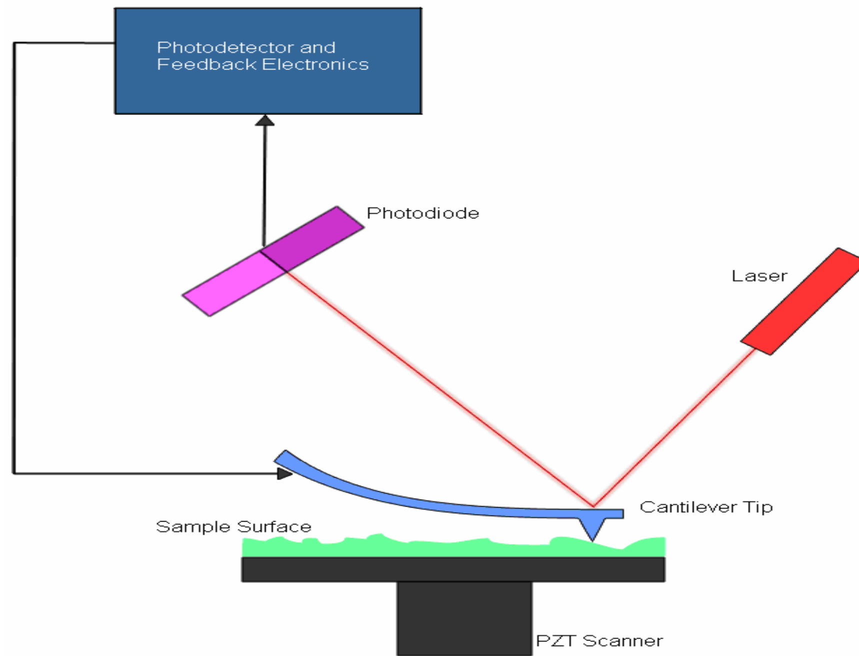

Figure 3.5 Schematic of Operation of an AFM [33]

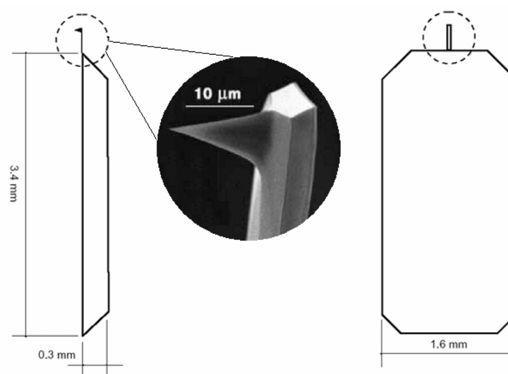

Figure 3.6 SEM Image/Schematic of an AFM Cantilever Tip [42]

3.5.3 Scanning Electron Microscopy (SEM)

The scanning electron microscope (SEM) is used to produce high resolution images of high magnification upto atomic level. In a SEM electrons are thermionically emitted from tungsten which acts as a cathode and are accelerated towards an anode; alternatively electrons can be emitted via field emission (FE). The electron beam, which typically has an energy ranging from a few 100 eV to 50 keV, is focused by one or two condenser lenses into a beam with a very fine focal spot sized in the order of 1 nm to 5 nm. The electron beam then passes through a pair of scanning coils in the objective lens, which deflect the beam in a raster fashion over a rectangular area of the sample surface. As the primary electrons strike the surface they are inelastically scattered by atoms in the sample. Through these scattering events, the primary electron beam effectively spreads and fills a teardrop-shaped volume, known as the interaction volume, extending from less than 100 nm to around 5 μm into the surface. Interactions in this region lead to the subsequent emission of electrons which are then detected to produce an image [33]. Figure 3.7 shows the basic block diagram of a scanning electron microscope.

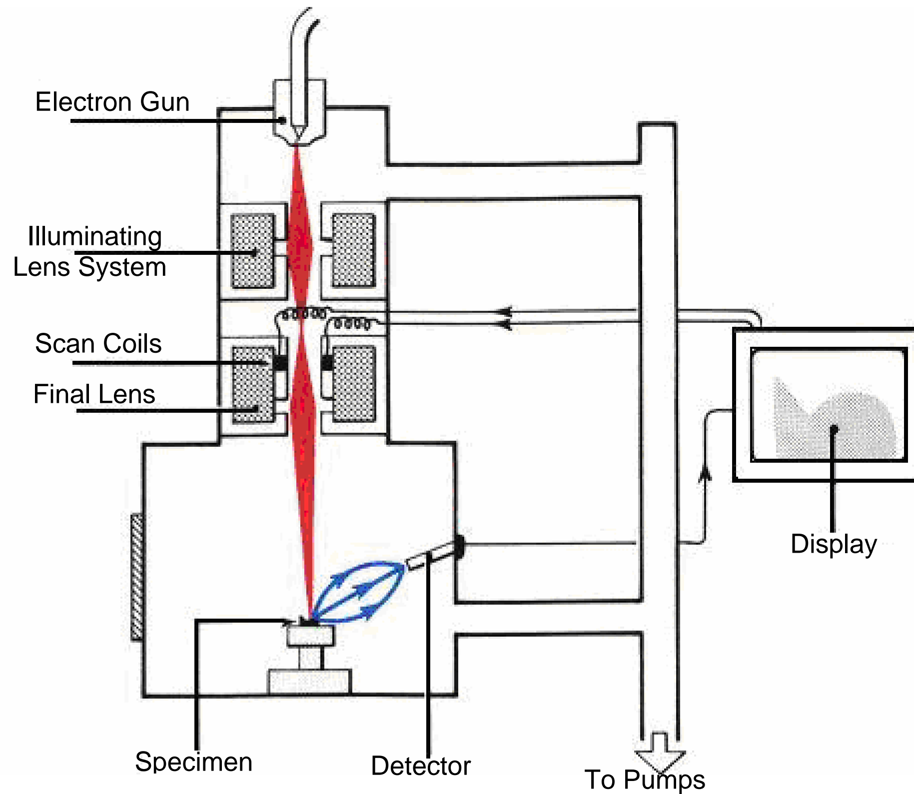

Figure 3.7 Block Diagram Showing the Operation of a SEM [43]

3.5.4 Dynamic Mechanical Analysis (DMA)

Dynamic mechanical analysis (DMA) is a technique that is used to study and characterize materials. The DMA technique is mostly used for observing the viscoelastic nature of polymers. An oscillating force is applied to a sample of material and the resulting displacement of the sample is measured, from which the stiffness of the sample can be determined, and the sample modulus can be calculated. The damping properties of the material can be determined by measuring the time lag in the displacement compared to the applied force.

Polymers with viscoelastic properties typically exist in two distinct states. These polymers exhibit the properties of a glass (high modulus) at low temperatures and those of a rubber (low modulus) at higher temperatures. This change of state, the glass

transition or alpha relaxation, can be observed during DMA run by scanning the temperature. The DMA technique is most widely used to investigate viscoelastic properties of CMP polishing pads as it can yield better data and can also be used to investigate the frequency dependant nature of the glass transition [33]. The DMA operation of DMA is based on the equation 3.2 [44]:

$$G^* = G' + iG'' \tag{3.2}$$

Where G* is the complex modulus, G" is loss modulus, i is imaginary root of -1 and G' is storage modulus. Storage modulus (G') gives the elastic properties of the material and is measured directly. The loss modulus factor (iG") gives the details about the viscous properties of the material. The ratio of loss modulus to storage modulus gives the tan delta or the damping ratio [45].

The DMA were performed using a DMA 2980 in the single cantilever bending mode. The pad samples were fixed using the DMA fixture clamps. The polyurethane pad samples with dimensions of 21.93x5.2x1.32 mm (pad A) and 21.83x5.75x1.37 mm (pad B) were tested using a multi frequency deformation mode at frequencies ranging from 1 – 100 Hz. The temperature was increased at a rate of 5 ºC/min and was tested from -150 ºC to 100 ºC. The samples were tested in the tension mode and liquid nitrogen was used for sub-ambient testing. Generally, in a DMA test storage modulus (G'), loss modulus (G") and tan delta (tanδ) are measured. Figure 3.8 shows the picture of the DMA 2980 instrument at USF.

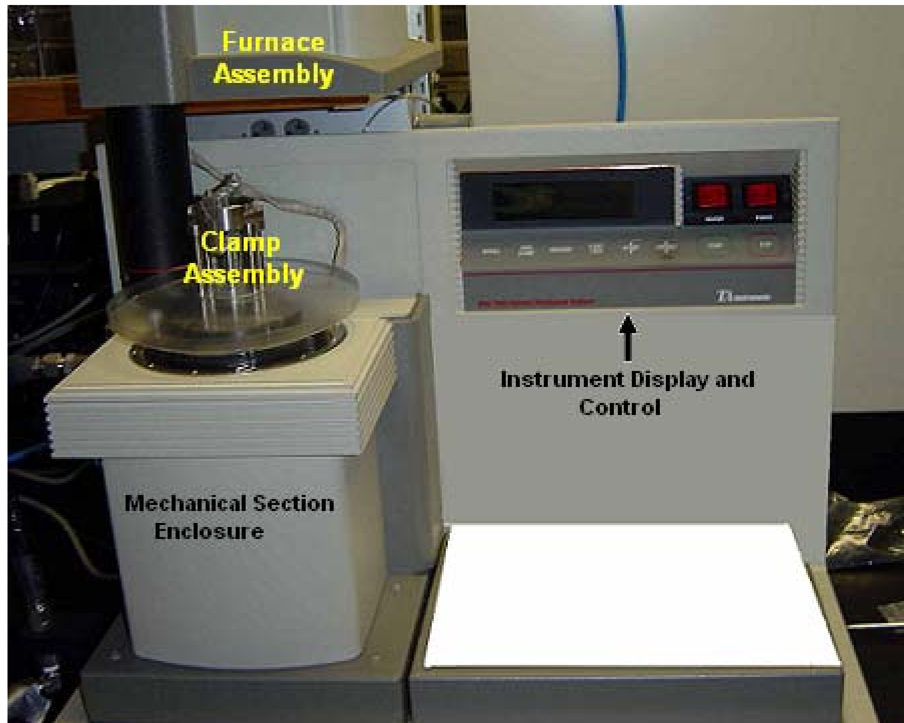

Figure 3.8 DMA 2980 Instrument at USF [48]

3.5.5 X-Ray Diffraction (XRD)

X-rays are electromagnetic radiation similar to light, but with a much shorter wavelength. They are produced when electrically charged particles of sufficient energy are decelerated. Typically in an X-ray tube, the high voltage maintained across the electrodes draws electrons toward a metal target. X-rays are produced at the point of impact, and radiate in all directions. [42]

If an incident X-ray beam encounters a crystal lattice, general scattering occurs. Although most scattering interferes with itself and is eliminated, diffraction occurs when scattering in a certain direction is in phase with scattered rays from other atomic planes. Under this condition the reflections combine to form new enhanced wave fronts that mutually reinforce each other. The relation by which diffraction occurs is known as the

Bragg law or equation. Because each crystalline material has a characteristic atomic structure, it will diffract X-rays in a unique characteristic pattern. The characterization of material structure using X-ray diffraction follows the Bragg's law described below:

$$n\lambda = 2d_s Sin\theta \quad (3.3)$$

Where d is lattice interplanar spacing of the crystal, Θ is X-ray incident angle, λ is wavelength of characteristic X-rays. The basic geometry of an X-ray diffractometer (fig. 3.9) involves a source of monochromatic radiation and an X-ray detector situated on the circumference of a graduated circle centered on the specimen. Divergent slits, located between the X-ray source and the specimen, and divergent slits, located between the specimen and the detector, limit scattered (non-diffracted) radiation, reduce background noise, and collimate the radiation. [42]

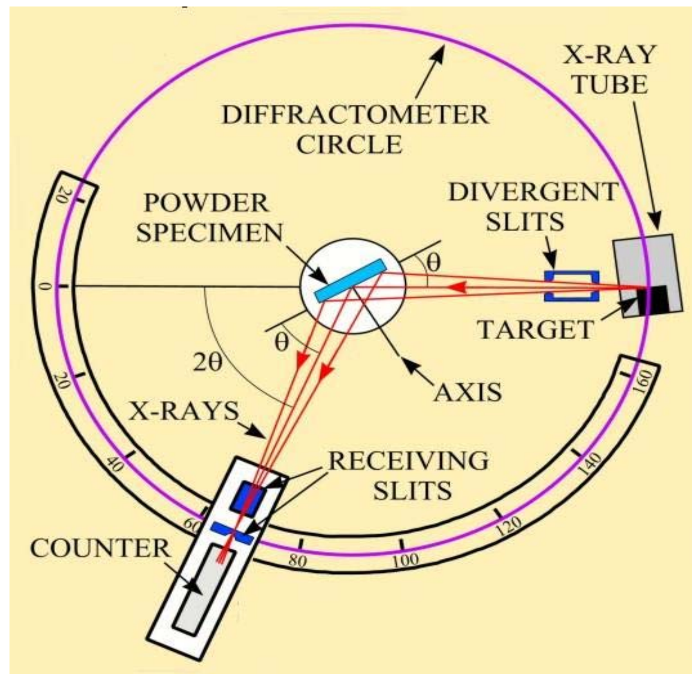

Figure 3.9 Schematic of an X-Ray Diffractometer. [51]

The detector and specimen holder are mechanically coupled with a goniometer so that a rotation of the detector through 2x degrees occurs in conjunction with the rotation of the specimen through x degrees, a fixed 2:1 ratio. A curved-crystal monochromator containing a graphite crystal is normally used to ensure that the detected radiation is monochromatic. When positioned properly just in front of the detector, only the Kα radiation is directed into the detector, and the Kß radiation, because it is diffracted at a slightly different angle, is directed away.

3.6 Summary

The CMP tool used for the experiments closely imitates large wafer fabrication production processes. The CMP tester generates real time lateral and normal force data. These signals can be monitored and analyzed in-situ. The polishing experiments were carried on CETR Cp-2 bench top polisher. The patterned copper samples were polished at different slurry temperatures keeping the pressure and velocity throughout the experiments. Two different kinds of pads and one type of polishing slurry were used for polishing experiments. The patterned copper samples polished at different condition were analyzed for the amount of dishing and erosion using atomic force microscopy (AFM) and profilometer. The change in pad physical properties with increase in temperature was analyzed using dynamic mechanical analysis (DMA). The surface morphology of the pad before and after conditioning was analyzed using scanning electron microscopy (SEM). The pad roughness before and after conditioning was measured using the profilometer. The structural changes in the copper blanket films was analyzed using X-Ray diffraction (XRD) analysis method for any change in crystallinity after polishing at different temperatures.

Chapter 4

Results and Discussion

The values of coefficient of friction COF and removal rates at different slurry temperatures were monitored and analyzed in-situ. The removal rate was calculated using the change in coefficient of friction (COF). The amount of dishing and metal loss during polishing was analyzed using profilometer and atomic force microscope (AFM). The change in pad physical properties with change in temperature was analyzed using dynamic mechanical analysis (DMA) technique.

4.1 Dynamic Mechanical Analysis (DMA) of Pads

The CMP polishing pad is subjected to high temperatures due to friction as a result of interaction between the polishing pad and wafer surface. This rise in temperature is partially brought down due to slurry flow. Tregub et al had investigated the effect of rise in temperature due to friction. The studies showed that there is a temperature rise in the order of about 20 °C to 30 °C during CMP [46]. During the polishing process the local pad temperature can increase significantly, especially at the point of contacts between the trench edges and pad. The substantial increase in the pad temperature during the CMP process can change the physical and mechanical properties of the pad.

The pads used for this research were analyzed using DMA in a frequency range of 1 to 100 Hz. Figure 4.1 shows the storage modulus and tan delta of the two polishing pads at different temperatures. It could be seen that in the temperature range between 15

°C to 35 °C the storage modulus decreased by 27 % for pad A and by around 50 % for pad B. The decrease in the storage modulus as seen from figure 4.1, results in the change of pad hardness and as such the pad polishing performance [47].

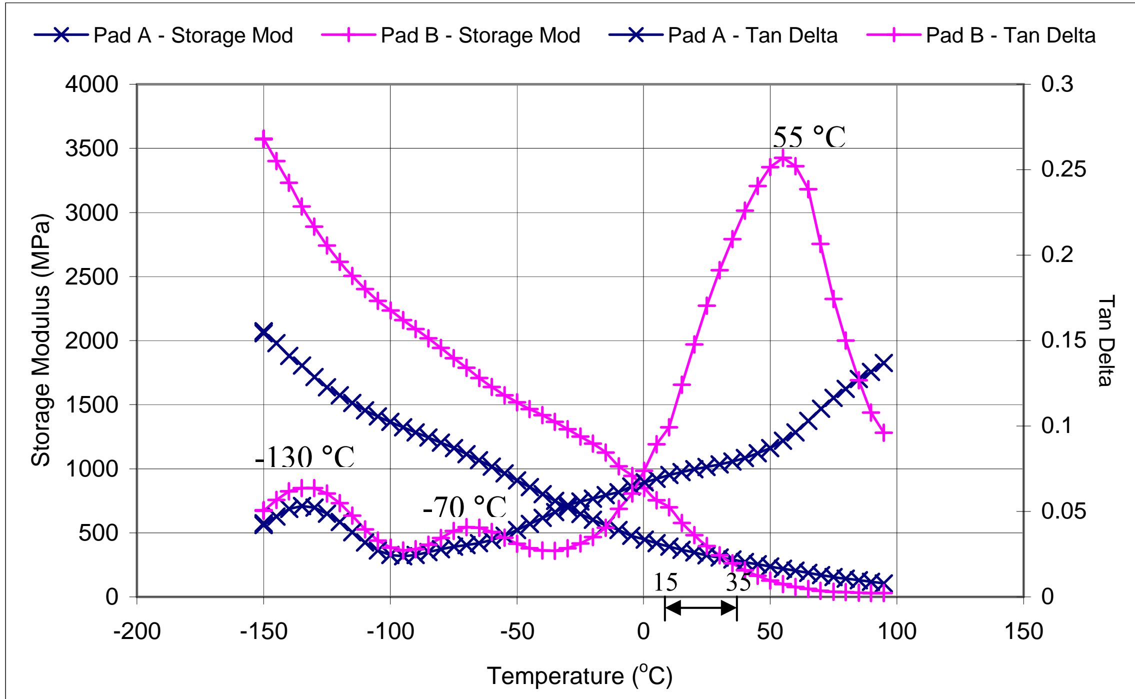

Figure 4.1 Storage Modulus and Tan Delta vs. Temperature at 10 Hz Frequency

In an ideal situation a polishing pad should show no change in the storage modulus within the range of operating temperature. With the increase in temperature the pad material softens and exhibits lower storage modulus. The change in percentage of storage modulus within the operating temperature shows that with increase in temperature pad B softens more quickly than pad A. The tan delta (tan δ) gives the energy dissipation of the pad materials. The peaks from the tan δ give the information about the transition temperature (Tg). It could be seen that pad A and pad B have sub-ambient transitions at -130 ºC and -130 ºC, -70 ºC respectively. Also pad B has a sharper transition at 55 ºC in tan δ, whereas pad A doesn't show any peaks below 100 ºC. This

sharp peak represents the glass transition temperature (Tg). The glass transition temperature represents a major transition, such as change in physical properties drastically as the material goes from hard glassy to a rubbery state. It could be interpreted that as the temperature increases pad B loses its physical properties drastically as compared to pad A. Thus, it could be stated that with in increase in temperature over the operating range pad B becomes softer than pad A, loses its stiffness.

The area under the tan δ gives the ability of the pad to absorb the mechanical energy or its toughness. Figure 4.2 shows the change in loss modulus with change in temperature. The loss modulus (G") is the product of the storage modulus (G') and tan δ.

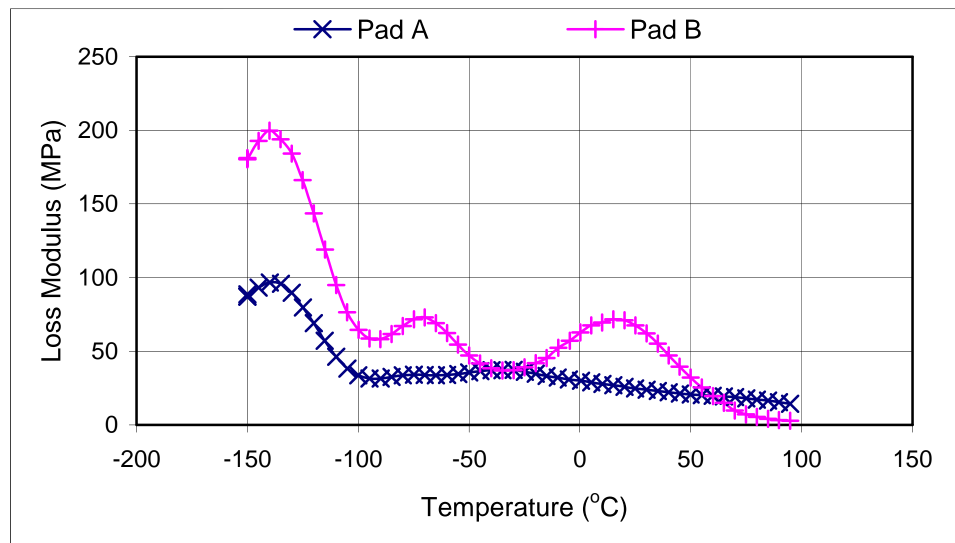

Figure 4.2 Loss Modulus vs. Temperature at 10 Hz Frequency

4.2 Scanning Electron Microscopy (SEM) Analysis

The scanning electron microscopy (SEM) analysis was performed on both kinds of polishing pads, before and after condition for same amount of time. The SEM analysis gives the surface topography of the pad, which improves after the conditioning. The

pores present on the pad material open after the conditioning of the pad, enabling constant removal rate between sample to sample and also improves the uniformity in polishing within and also from wafer to wafer. Figures 4.3 and 4.4 show the pad A and pad B respectively, before and after conditioning.

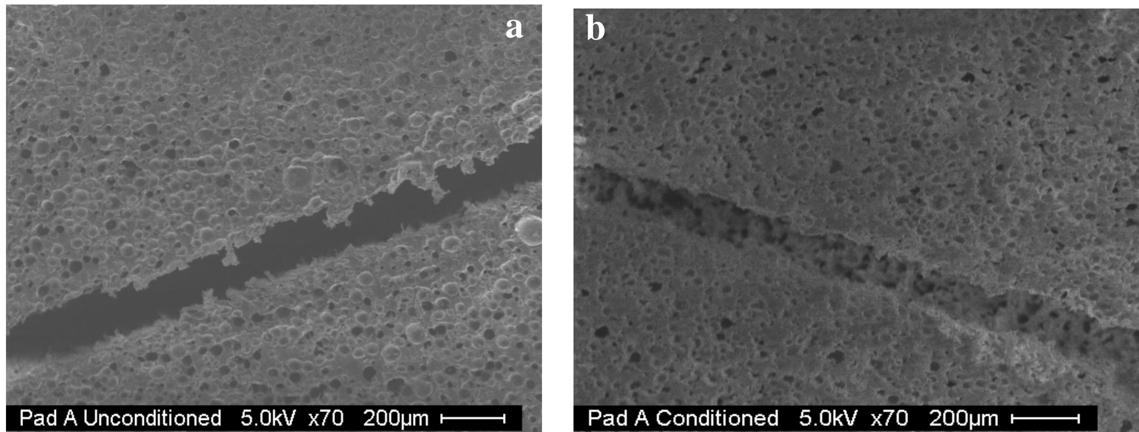

Figure 4.3 SEM Image of Pad A - a) Unconditioned b) Conditioned

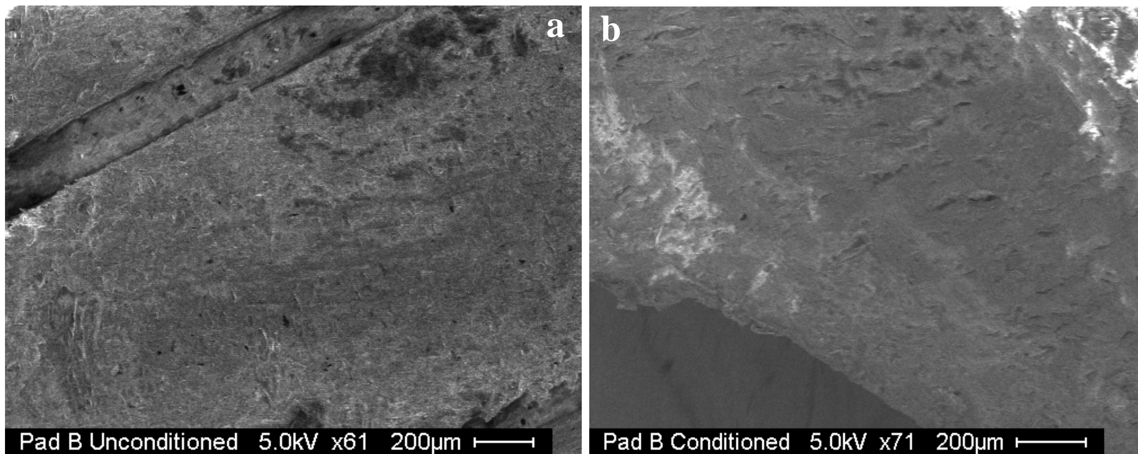

Figure 4.4 SEM Image of Pad B - a) Unconditioned b) Conditioned

From the figures it can be seen that the pas surface roughness improves after conditioning the pad. Also it can be seen that after conditioning more number of pores open up. With the increase in pas roughness after conditioning the same amount of

removal rate can be maintained from sample to sample and also the uniformity in polishing also increased with conditioning.

4.3 Analysis of COF and Removal Rate with Slurry Temperature and Pad

4.3.1 Coefficient of Friction (COF)

The patterned copper samples were polished at various process conditions as mentioned in table 3.1. The graphs of COF vs. polishing time at five different temperatures on pad A using two types of slurries are shown in figures 4.5 – 4.9.

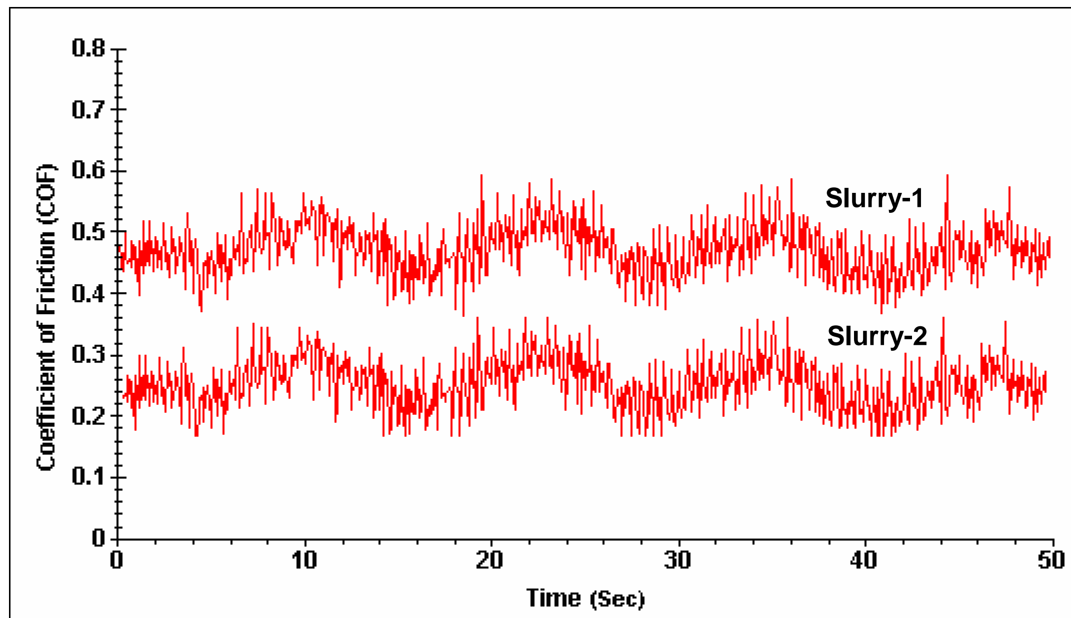

Figure 4.5 COF vs. Time of a Sample at 15 °C on Pad A

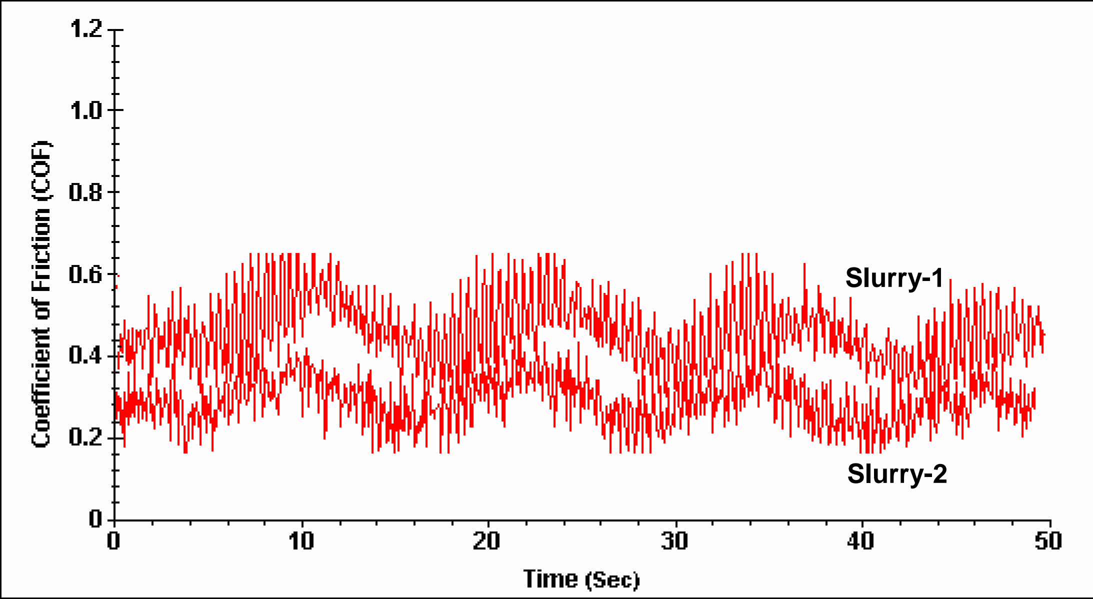

Figure 4.6 COF vs. Time of a Sample at 20 °C on Pad A

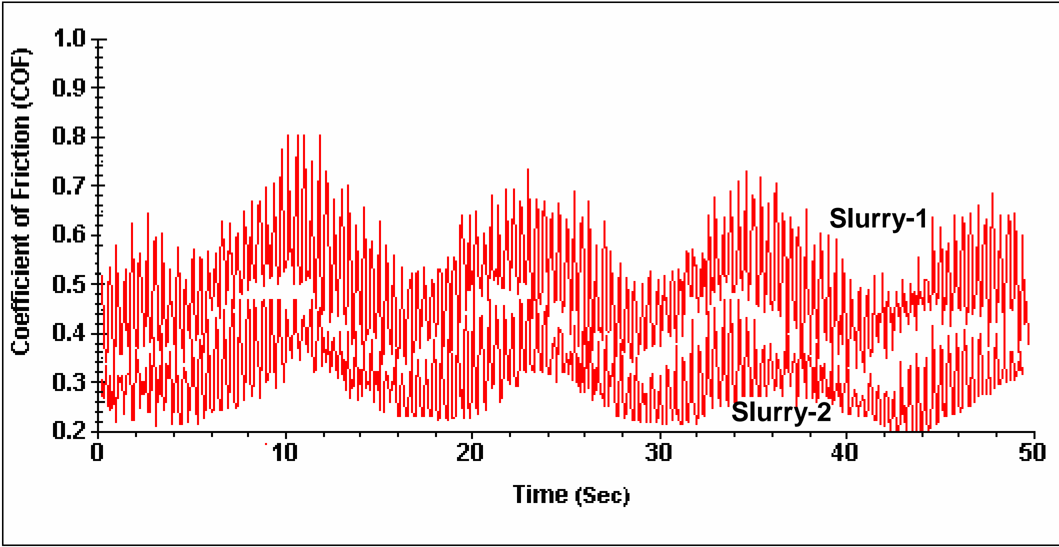

Figure 4.7 COF vs. Time of a Sample at 25 °C on Pad A

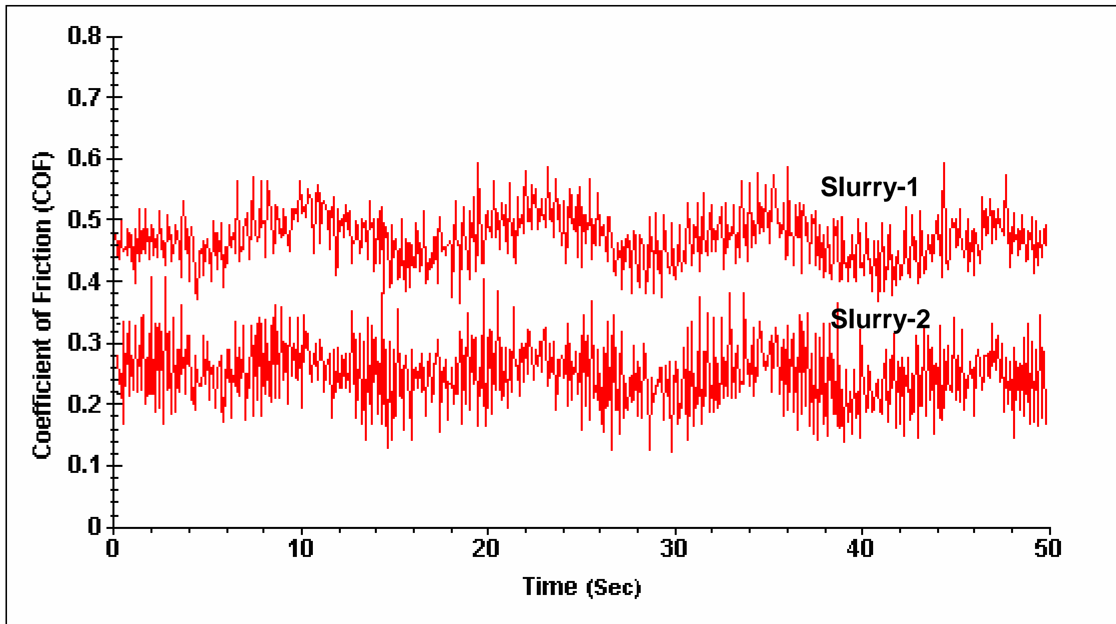

Figure 4.8 COF vs. Time of a Sample at 30 °C on Pad A

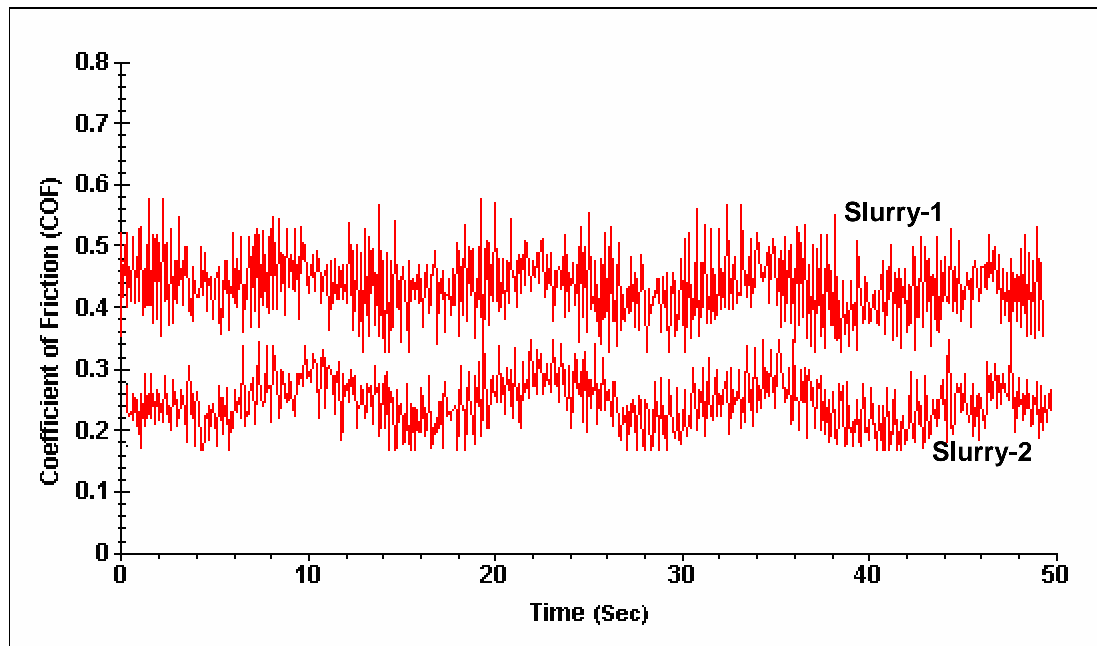

Figure 4.9 COF vs. Time of a Sample at 35 °C on Pad A

The influence of slurry temperature on the removal rate and coefficient of friction (COF) was analyzed. The change in the COF with change in slurry temperature is

presented in graphs above. The graphs of COF vs. polishing time at five different temperatures and using two types of slurries on pad B are shown in figures 4.10 – 4.14.

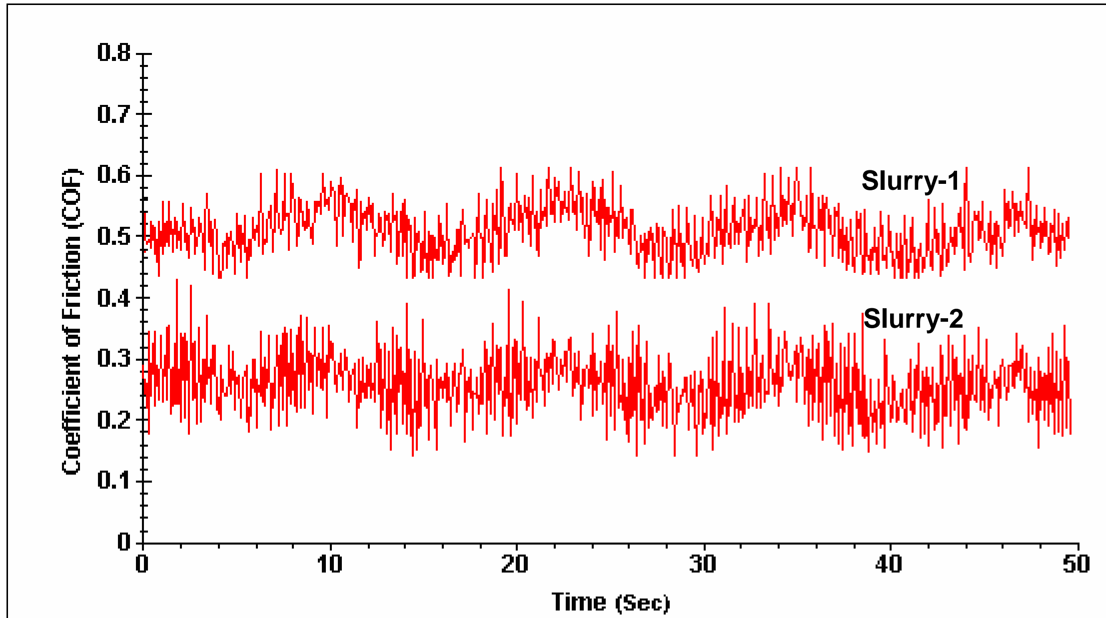

Figure 4.10 COF vs. Time of a Sample at 15 °C on Pad B

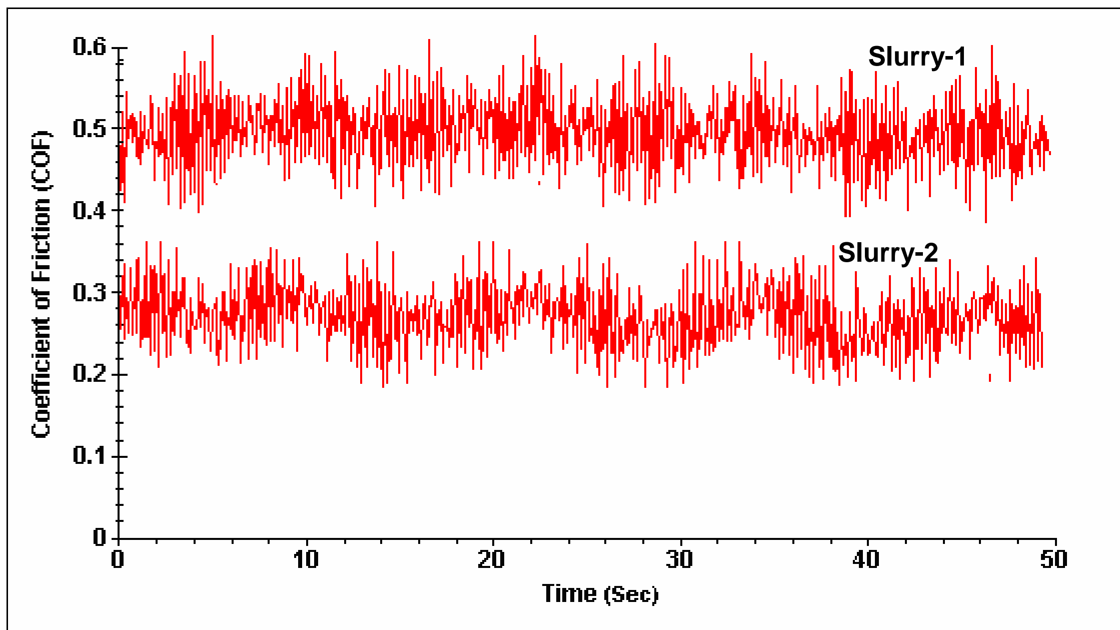

Figure 4.11 COF vs. Time of a Sample at 20 °C on Pad B

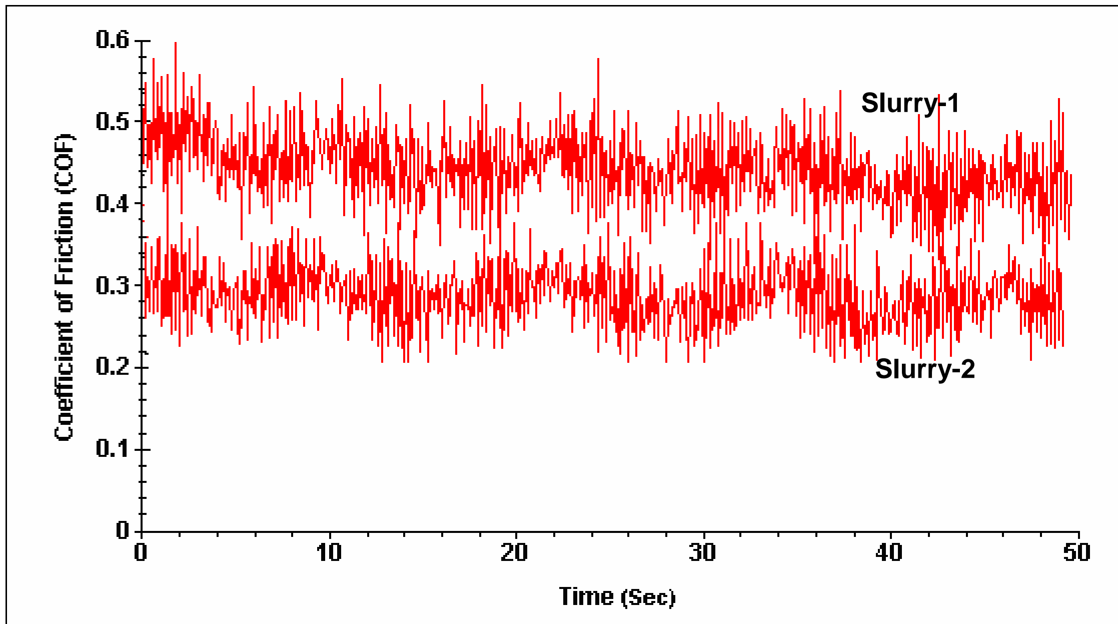

Figure 4.12 COF vs. Time of a Sample at 25 °C on Pad B

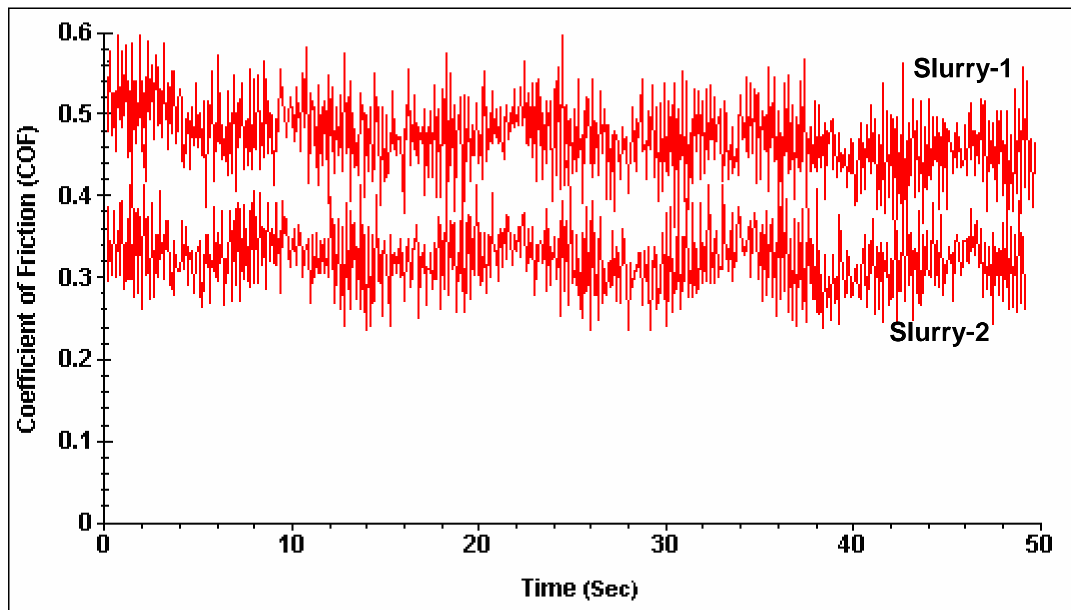

Figure 4.13 COF vs. Time of a Sample at 30 °C on Pad B

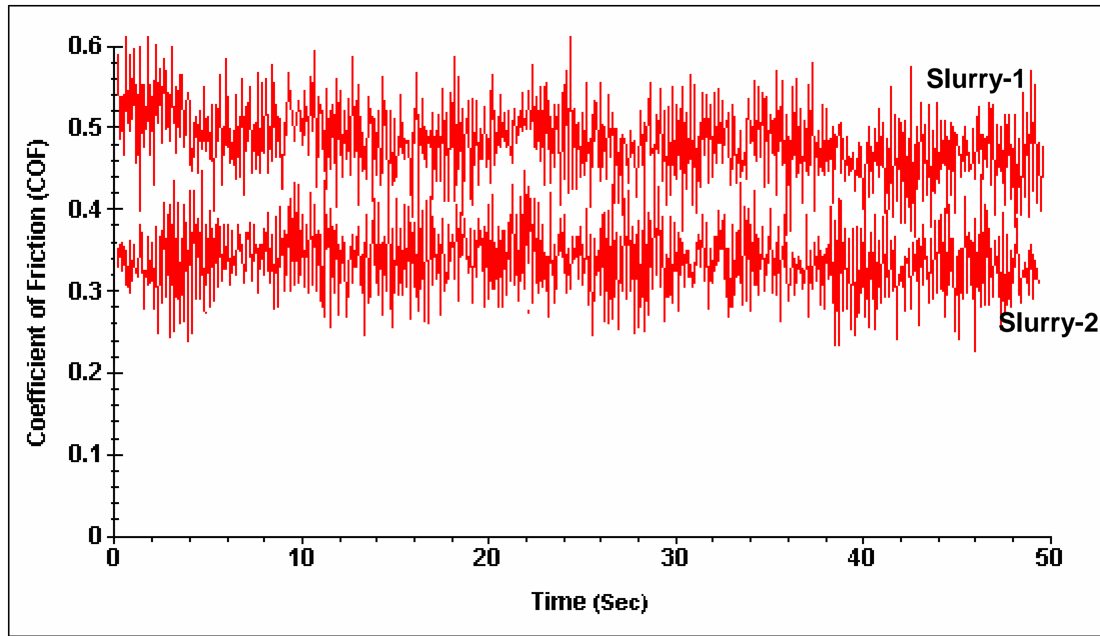

Figure 4.14 COF vs. Time of a Sample at 35 °C on Pad B

Table 4.1 and 4.2 show the COF values of samples polished at five different slurry temperatures on two pads (pad A and pad B) and two slurries. Three replicates of samples were taken at each slurry temperature. The average of the three replicates was taken to plot the COF vs. slurry temperature graph. Figure 4.15 and 4.16 show the graphs between COF at five different slurry temperatures taken on two different polishing pads and using slurry 1 and slurry 2 respectively.

Table 4.1 Coefficient of Friction at Different Slurry Temperatures Using Slurry-1

		15 ºC	20 ºC	25 ºC	30 ºC	35 ºC
COF on Pad - A	1	0.4682	0.4822	0.4824	0.4856	0.4878
	2	0.4785	0.4751	0.4821	0.4864	0.4872
	3	0.4587	0.4736	0.4795	0.4803	0.4869
	Average	0.4675	0.4769	0.4813	0.4841	0.4873
COF on Pad - B	1	0.5048	0.5136	0.5199	0.5337	0.5449
	2	0.5039	0.5143	0.5218	0.5348	0.5441
	3	0.5044	0.5127	0.5228	0.5341	0.5435
	Average	0.5043	0.5135	0.5215	0.5342	0.5441

Table 4.2 Coefficient of Friction at Different Slurry Temperatures Using Slurry-2

		15 ºC	20 ºC	25 ºC	30 ºC	35 ºC
COF on Pad - A	1	0.2241	0.2501	0.253	0.2607	0.2711
	2	0.2446	0.2495	0.2514	0.2597	0.2704
	3	0.2457	0.2498	0.2527	0.2601	0.2709
	Average	0.2448	0.2498	0.2523	0.2601	0.2708
COF on Pad - B	1	0.2897	0.2951	0.3031	0.3217	0.3431
	2	0.2888	0.2937	0.3025	0.3221	0.3425
	3	0.2894	0.2937	0.3021	0.3211	0.3425
	Average	0.2893	0.2941	0.3025	0.3216	0.3427

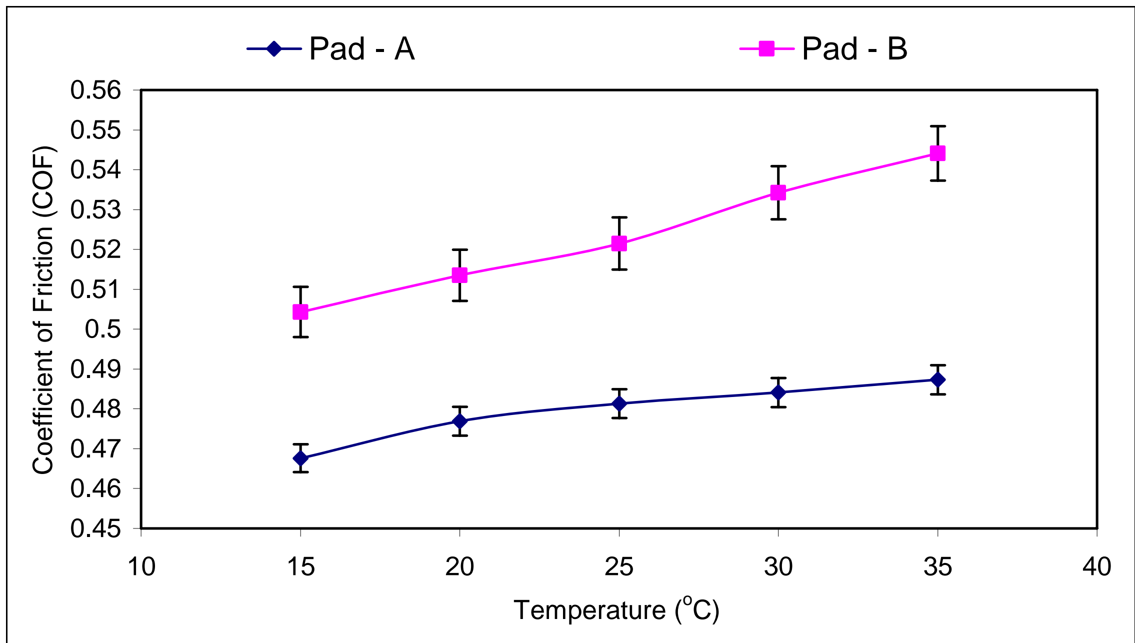

Figure 4.15 Change in COF vs. Slurry Temperature for Slurry - 1

From tables 4.1, 4.2 and figures 4.15, 4.16 it can be seen that for pad B the coefficient of friction (COF) increases with increase in slurry temperature with both slurries. For pad A the change in COF with increase in slurry temperature is very minimal for both slurries. This change in coefficient of friction can be attributed to increased area of contact of pad-wafer surface with increase in slurry temperature, resulting in higher

shear force at the interface, which can be supported by the change in COF with change in temperature (see fig. 4.15). The change in coefficient of friction during CMP employing pad 2 was found to be higher compared to pad A, which can be explained by the DMA analysis (see fig. 4.1) that with increase in temperature there is a change in pad hardness and material characteristics, resulting in increased area of contact. It can be seen that of the two pads used the second pads undergoes changes at a lower temperature and does expand elastically, explaining the reason behind the higher COF on one of the pads used.

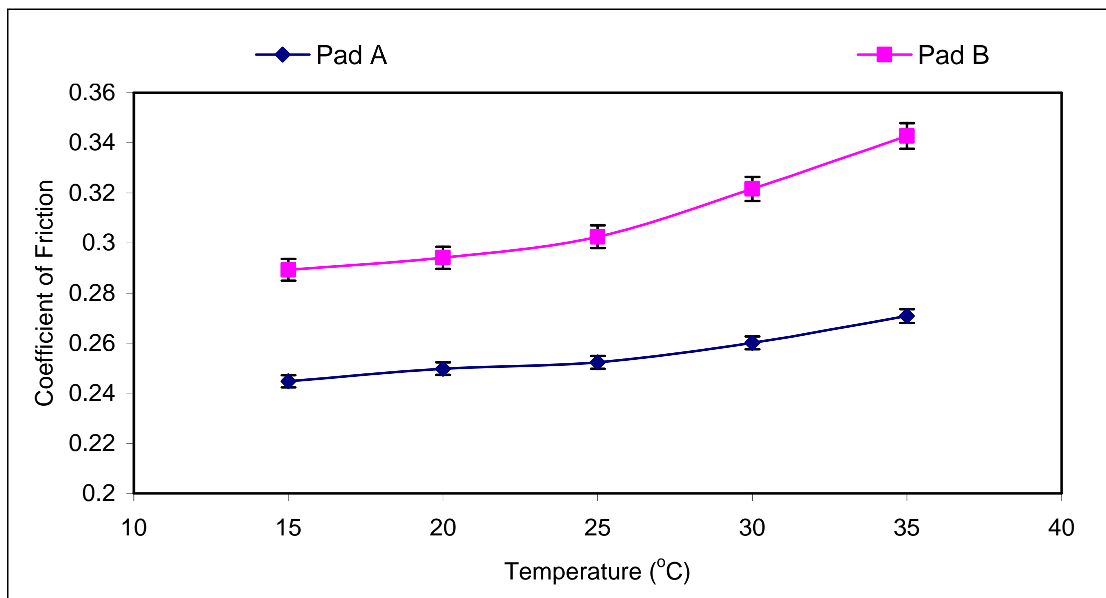

Figure 4.16 Change in COF vs. Slurry Temperature for Slurry – 2

4.3.2 Removal Rate

Tables 4.3 shows the removal rate of patterned copper samples polished at five slurry temperatures on two different slurries. Three replicates of removal rate (nm/min) of copper samples were taken at each slurry temperature. The average of the three replicates was taken to plot the removal rate vs. slurry temperature graph. Figures 4.17

and 4.18 shows the graphs between removal rates at three different slurry temperatures taken on two different polishing pads.

Table 4.3 Removal Rates at Different Slurry Temperatures Using Slurry 1 and 2

		15 ºC	20 ºC	25 ºC	30 ºC	35 ºC
Removal Rate on Pad - A (nm/min)	Slurry - 1	190.5	222.2	255.3	285.7	333.3
	Slurry - 2	137.9	153.8	160	173.9	218.2
Removal Rate on Pad - B (nm/min)	Slurry - 1	333.3	400	500	600	666.7
	Slurry - 2	153.8	181.8	200	222.3	272.7

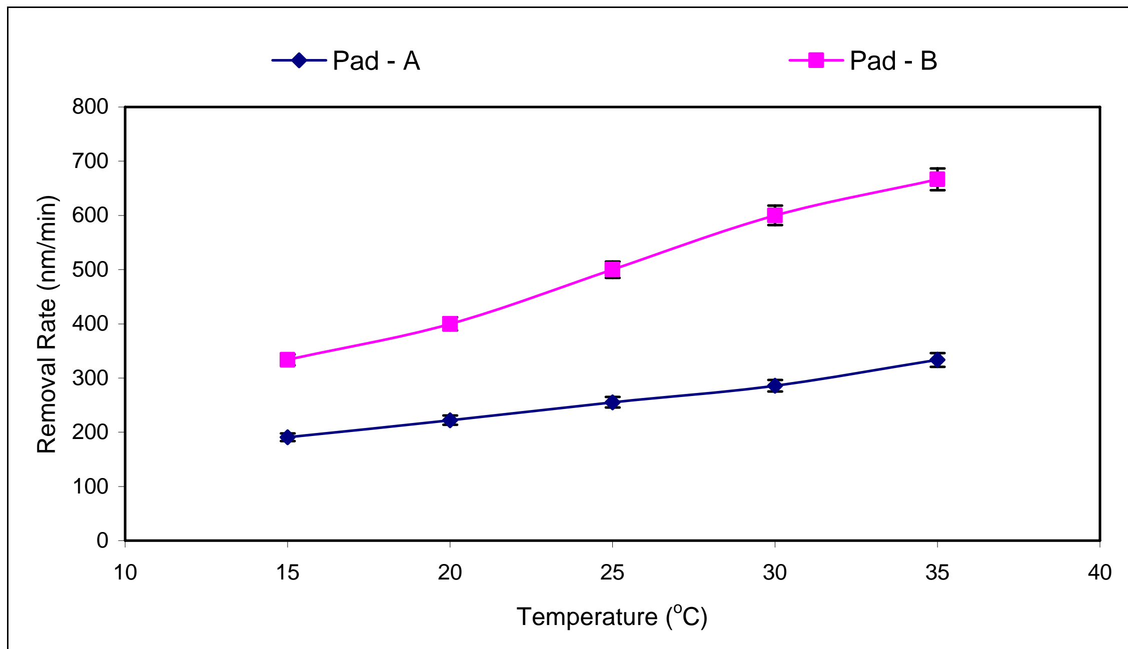

Figure 4.17 Removal Rate vs. Slurry Temperature Using Slurry-1

From table 4.3 and figures 4.17 and 4.18 it can be seen that removal rate increases with increase in slurry temperature for pad A and pad B polishing pads. The removal rate

of copper is higher on pad B compared to pad A. This variation in removal rates on two polishing pads can be attributed to pad hardness and other pad mechanical properties.

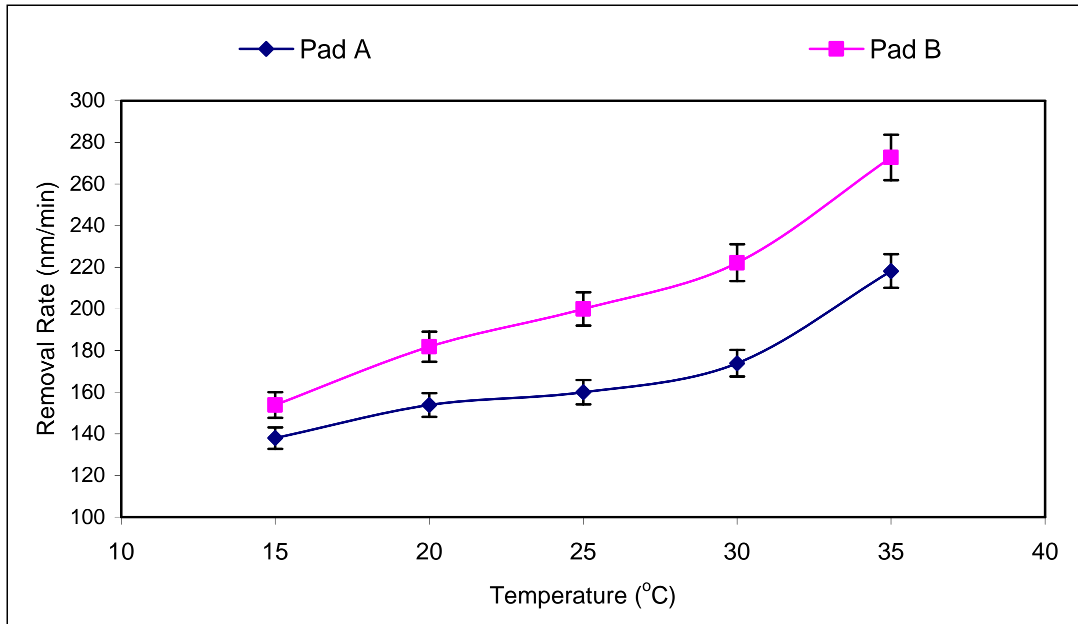

Figure 4.18 Removal Rate vs. Slurry Temperature Using Slurry-2

The increase in removal rate without any significant change in coefficient of friction during CMP using pad A is attributed mainly to the change in chemical reaction kinetics. Also it can be concluded that the changes in the mechanical properties of pad B are not influencing the tribological mechanism at the interface. The difference in the removal rates between the pads can be attributed to the difference in mechanical properties of pads such as hardness and storage modulus. Pad B was found to have higher removal rates with increase in temperature compared to pad A. The increase in removal rates and differences in removal rates on two types of polishing pads can be correlated with the coefficient of friction values, increase in COF aiding in increased removal rate along with increase in the metal dissolution rates with increase in slurry temperature. The

increase in the coefficient of friction and material removal rate with increase in slurry temperature compares well with literature [1].

4.4 Analysis of Dishing with Slurry Temperature and Pad

The patterned copper samples polished at five different slurry temperatures were analyzed for the amount of dishing on 10 µm, 20 µm and 50 µm wide metal lines and on 100 µm square bond pads using profilometer and atomic force microscopy (AFM). Table 4.4 gives the values of the normalized dishing data on the metal lines and the bond pads using two slurries. Figures 4.19 and 4.20 show the amount of dishing on a 10 µm wide metal line at different slurry temperatures on different pads using two slurries. The amount of dishing (nm) has been normalized for analysis.

Table 4.4 Normalized Dishing Data on Metal Lines and Bond Pads

	Slurry Temperature (ºC)	10 µm wide metal line		20 µm wide metal line		50 µm wide metal line		100 µm bond pads	
		Pad A	Pad B	Pad A	Pad B	Pad A	Pad B	Pad A	Pad B
Slurry - 1	15 ºC	0.0307	0.075	0.1194	0.1358	0.5881	0.5120	0.6336	0.481
	20 ºC	0.0848	0.114	0.1441	0.1619	0.7586	0.6003	0.7108	0.564
	25ºC	0.1364	0.1531	0.1839	0.191	0.8651	0.698	0.9132	0.651
	30ºC	0.1657	0.1868	0.2146	0.225	0.9098	0.8218	1	0.747
	35ºC	0.1502	0.1647	0.1927	0.2078	0.8825	0.7791	0.98	0.665
Slurry - 2	15ºC	0.0282	0.0986	0.0594	0.1425	0.483	0.8786	0.5204	1
	20ºC	0.0184	0.0804	0.0409	0.1146	0.4005	0.8199	0.2134	0.933
	25ºC	0.0116	0.0685	0.0294	0.0977	0.254	0.7981	0.167	0.889
	30ºC	0.0084	0.0525	0.0238	0.0746	0.1615	0.7779	0.1543	0.843
	35ºC	0.0078	0.035	0.020	0.0595	0.066	0.7592	0.1202	0.779

From table 4.3 and figure 4.19 it can be seen that the dishing on the 10 µm metal line increased with rise in slurry temperature from 15 ºC to 30 ºC and then decreased with further rise in slurry temperature to 35 ºC using slurry 1. The main reason for the change in dishing due to temperature can be attributed to the change in the properties of surface asperities of the pad with the change in slurry temperature.

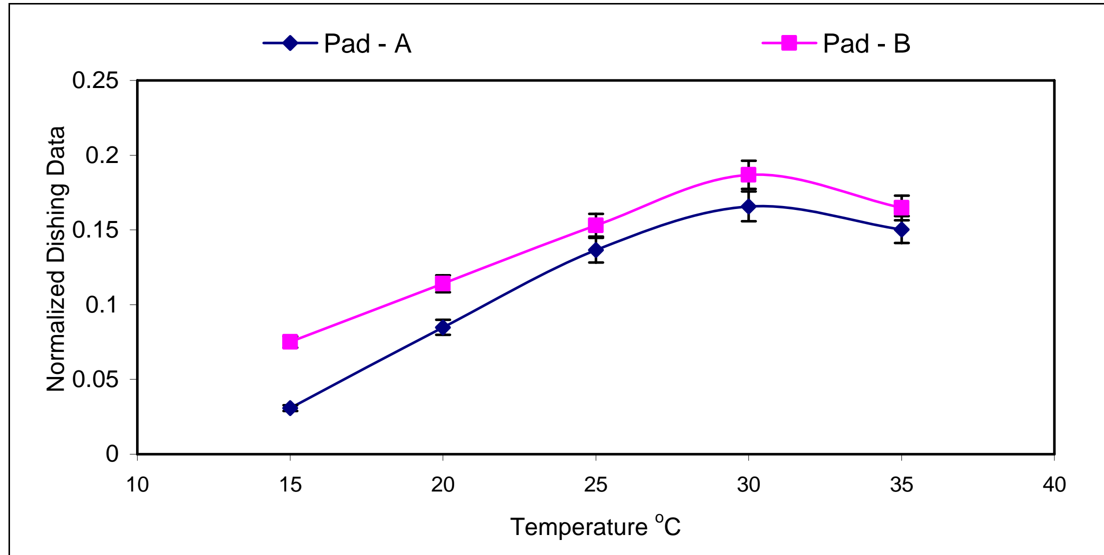

Figure 4.19 Dishing on a 10 µm Wide Metal Line vs. Slurry Temperature Using Slurry-1

Also with the increase in slurry temperature a change in chemical dissolution rate of copper [25] could be influencing the dishing characteristics. It can also be seen from figure 4.19 that amount of dishing is higher on pad B compared to pad A on certain features and vice versa on others. This difference in dishing characteristics as demonstrated by different pads suggests that there is more than one mechanism that can explain the dependence of dishing on rise in temperature. The high dishing on 10 µm on pad B compared to low dishing on pad A (fig 4.19) could be due to local softening of the pad because of relatively high temperatures at the interface. The asperities of a softer pad (pad B) reach deeper into the metal lines of smaller widths compared to the harder pads

(pad A), resulting in increase of dishing. This change in pad physical properties with increase in slurry temperature is well explained with the help of dynamic mechanical analysis (DMA) of polishing pad, presented in the following sections. From figure 4.20 it can be seen that the dishing values on two types of polishing pads decrease with increase in slurry temperature using slurry 2.

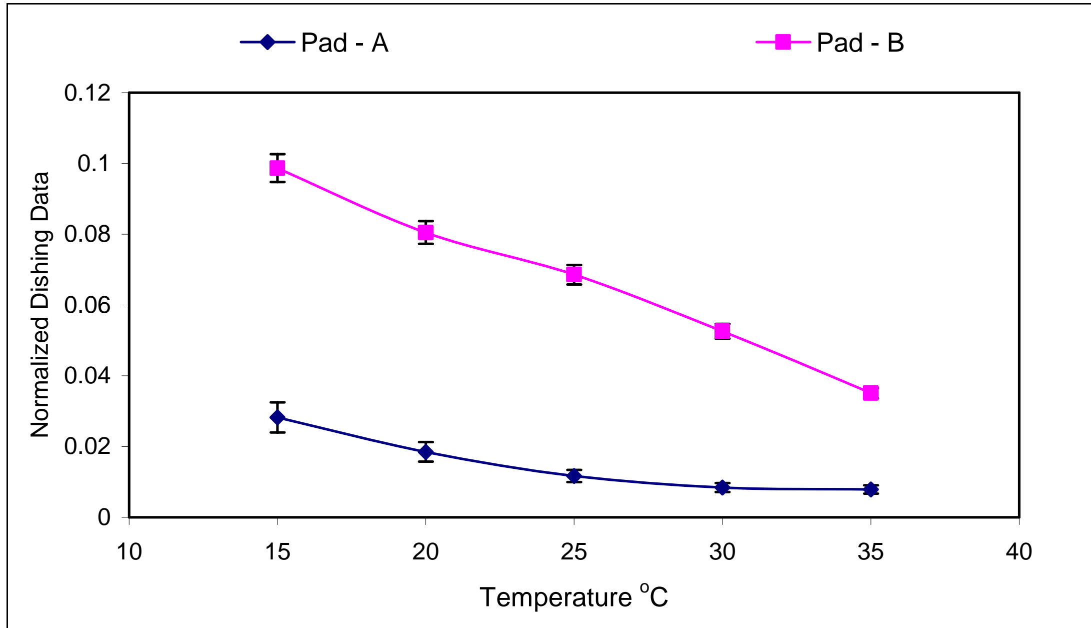

Figure 4.20 Dishing on a 10 μm Wide Metal Line vs. Slurry Temperature Using Slurry-2

This may be due to the reason that the slurry 2 had a different oxidizer (Ammonium per sulfate) and when compared with slurry -1 the oxidation rate is low and also reactivity's of both the slurries with pad is different. Also the chemical nature of the slurries is suspected to play an important role in determining the change in dishing with change in temperature. It can be noted that also with slurry 2 the pad B has higher amount of dishing when compared to pad A.

Figures 4.21 and 4.22 show the normalized dishing on a 20 μm wide metal line with increase in slurry temperature. However, as the line width increases, on a 20 μm

metal line (fig 4.21, 4.22) the amount of dishing increases with increase in line width compared to 10 µm interconnect line. As with the 10 µm interconnect line the dishing with pad B is higher than pad A on 20 µm interconnect line.

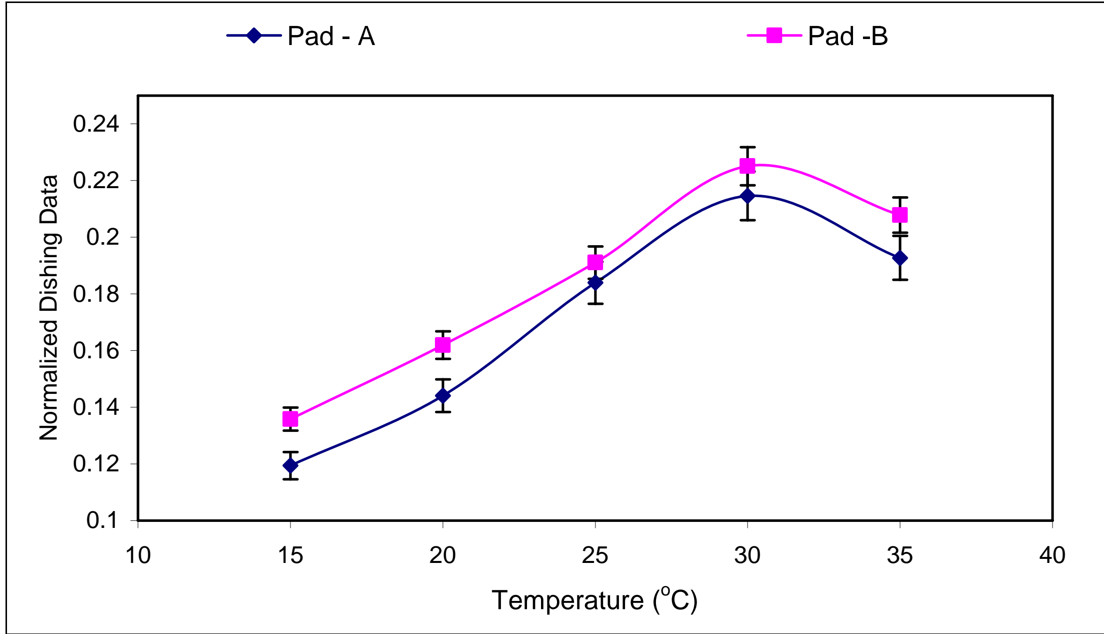

Figure 4.21 Dishing on a 20 µm Wide Metal Line vs. Slurry Temperature Using Slurry-1

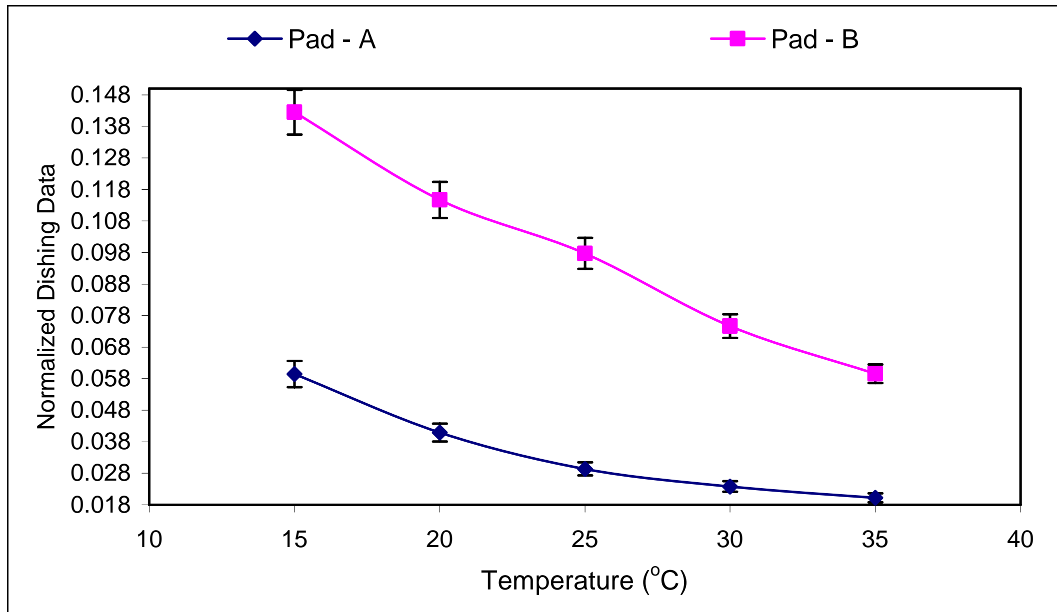

Figure 4.22 Dishing on a 20 µm Wide Metal Line vs. Slurry Temperature Using Slurry-2

Figures 4.23 and 4.24 show the normalized dishing on a 50 µm wide metal line with increase in slurry temperature. However, as the line width increases, on a 50 µm metal line (fig 4.23, 4.24) the amount of dishing increases with increase in line width compared to 10 and 20 µm interconnect lines. As compared with the 10 and 20 µm interconnect lines the dishing with pad A is higher than pad B on 50 µm interconnect line with slurry 1, but where as with slurry 2 the dishing with pad B is higher than pad A.

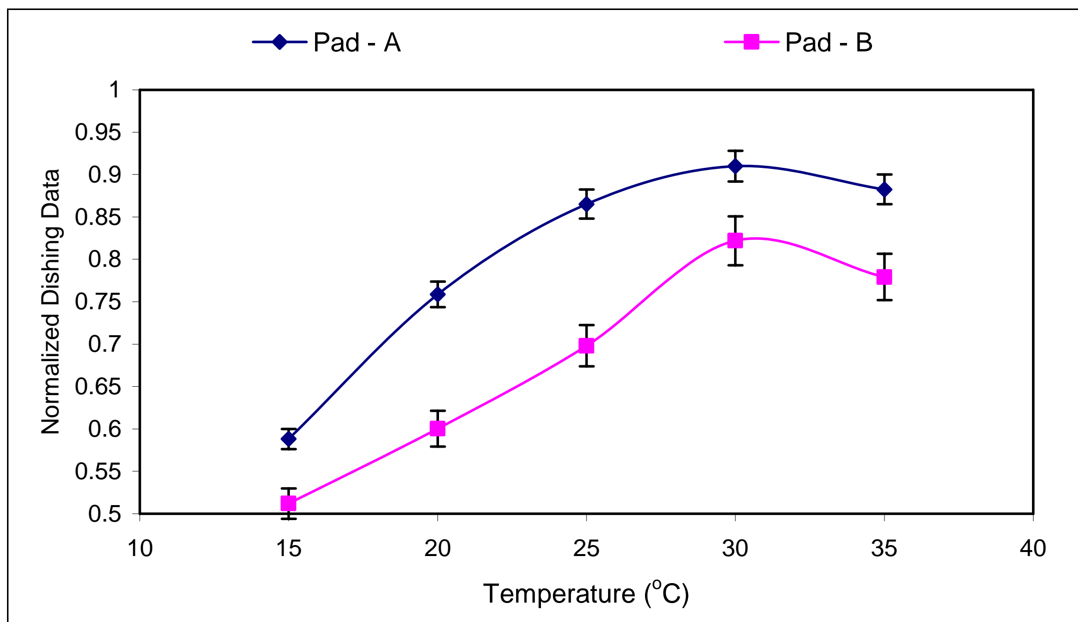

Figure 4.23 Dishing on a 50 µm Wide Metal Line vs. Slurry Temperature Using Slurry-1

This might be due to the reason that the pad asperities reaching deeper at higher temperature and also as pad A is stiffer than pad B, on larger line widths it might reach more deeper into the interconnect line cause more amount of dishing. With slurry 2 the pad B has dishing than pad A (see fig 4.24) and this might be due to the pad slurry interaction playing an important role. Thus this observation confirms that the amount of dishing changes with line width [1], nature of the pad and slurry. Also this confirms that the rather than only the effect of temperature there is a combinatorial effect of slurry

temperature, slurry type and pad on the dishing generated rather than the effect of only one single factor.

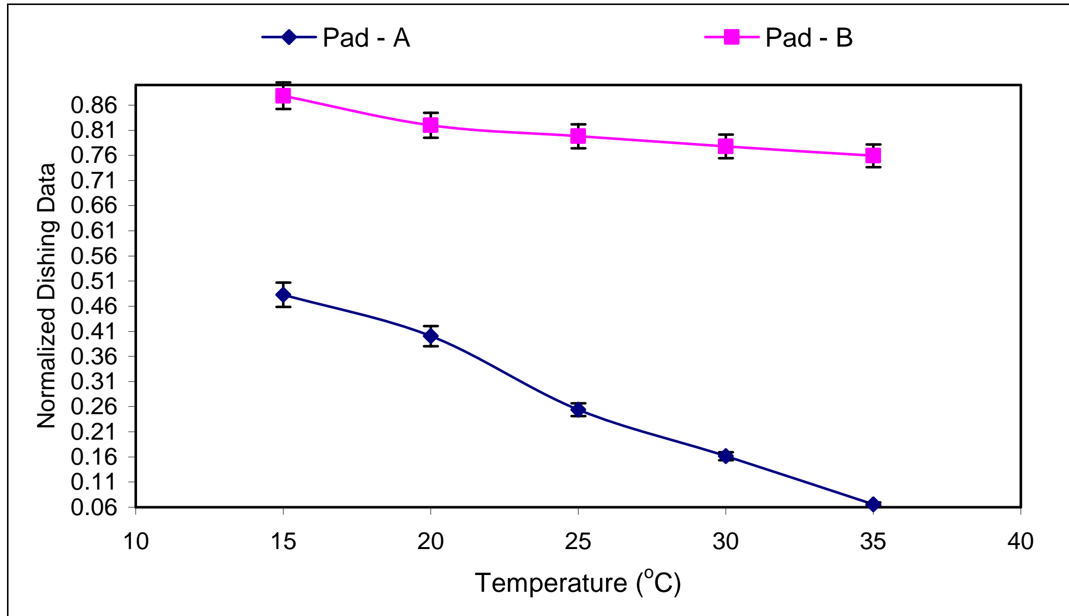

Figure 4.24 Dishing on a 50 μm Wide Metal Line vs. Slurry Temperature Using Slurry-2

Figures 4.25 and 4.26 shows the normalized dishing on a 100 μm bond pads with increase in slurry temperature using two slurries. The dishing increases with increase in temperature from 15 ºC to 30 ºC and then decreased with rise slurry temperature to 35 ºC using slurry 1, whereas with slurry 2 the amount of dishing decreases with increase in slurry temperature.

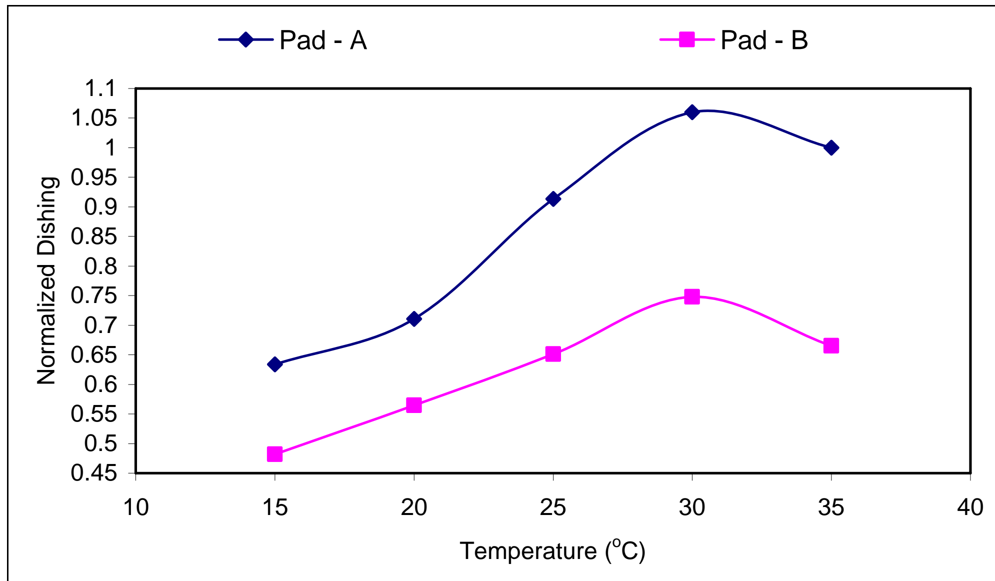

Figure 4.25 Dishing on a 100 µm Bond Pad vs. Slurry Temperature Using Slurry – 1

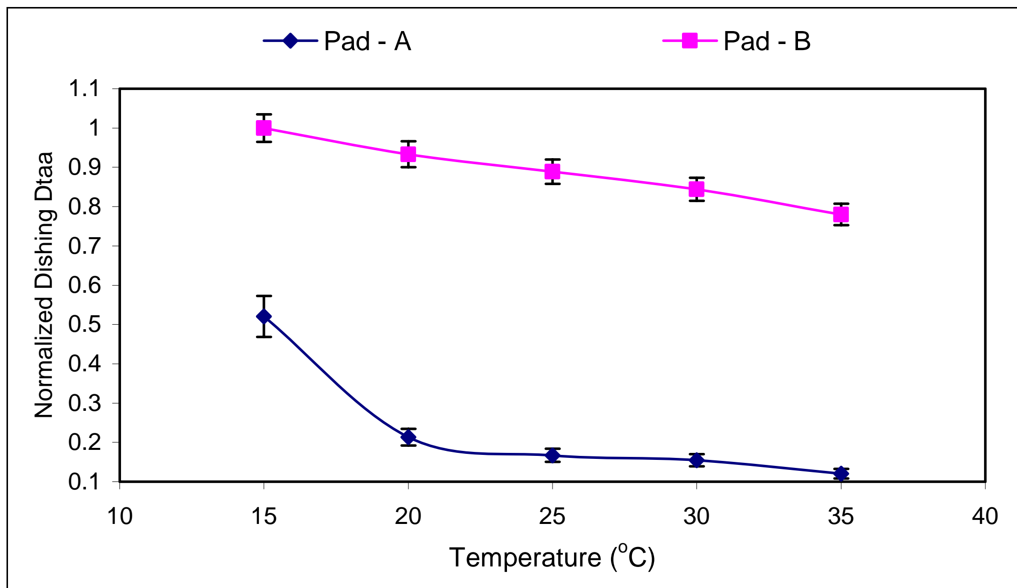

Figure 4.26 Dishing on a 100 µm Bond Pad vs. Slurry Temperature Using Slurry - 2

Dishing increases with increase in line width is also confirmed again. The above phenomenon shows that softer pads get into the smaller metal lines more easily than stiffer or harder pads and cause more defects. Pad B which is less stiffer in nature

compared to pad A, confirmed by the DMA analysis tends to get into smaller metal lines and removes more amount material than pad A. With increase in line widths pad A gets easily into metal lines and removes more amount of material even though pad B also gets into metal lines because due to the softer nature of pad B it causes less amount of dishing. Figure 4.27 shows the atomic force microscope (AFM) dishing profiles of metal lines of different widths.

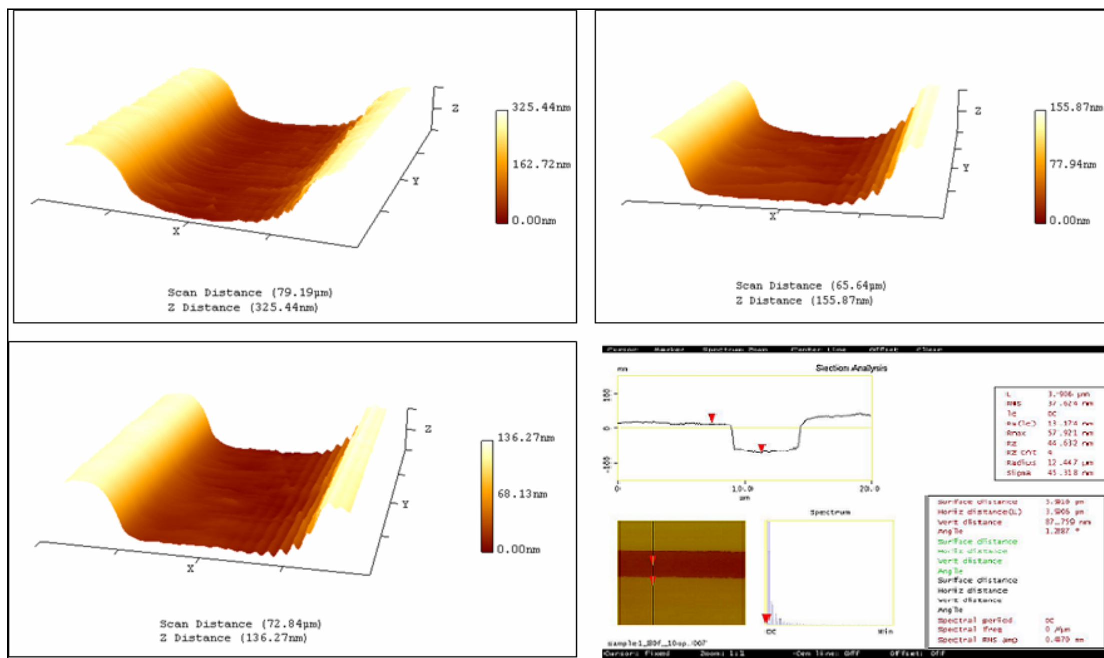

Figure 4.27 Dishing Profiles of Metal Lines of Different Widths

4.5 Analysis of Metal Loss with Slurry Temperature and Pad

The patterned copper samples polished at different slurry temperatures were analyzed for the amount of metal loss on metal lines of 100 µm line width and 99 % pattern density as a function of slurry temperature and pad type using profilometer and atomic force microscopy (AFM). Figures 4.28 and 4.29 show the metal loss at different slurry temperatures on two types of polishing pads using two types of polishing slurries.

It can be seen from figure 4.28 that the amount of metal loss is higher with pad A than with pad B. The area of the feature on which the metal loss was measured has dimensions in the order of 1500 μm. The reason for higher metal loss with pad A could be that the reaching of asperities of pad A well into the metal lines as well as the dielectric material is the dominating factor as compared to the hardness of the pad. From this we can infer that pad asperity interaction with the feature and the bulk hardness of the pad both have a combinatorial effect on dishing.

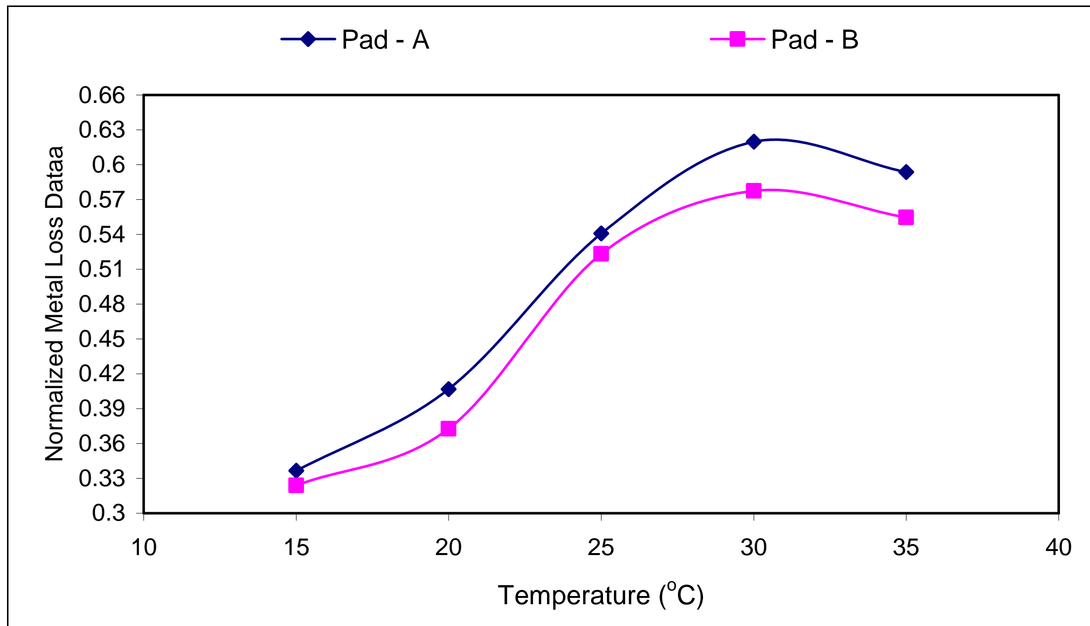

Figure 4.28 Metal Loss vs. Slurry Temperature Using Slurry - 1

Figure 4.29 shows the metal loss on the two types of polishing pads using slurry 2. The amount of metal loss decreases with increase in slurry temperature, pad B having more amount of metal loss than pad A

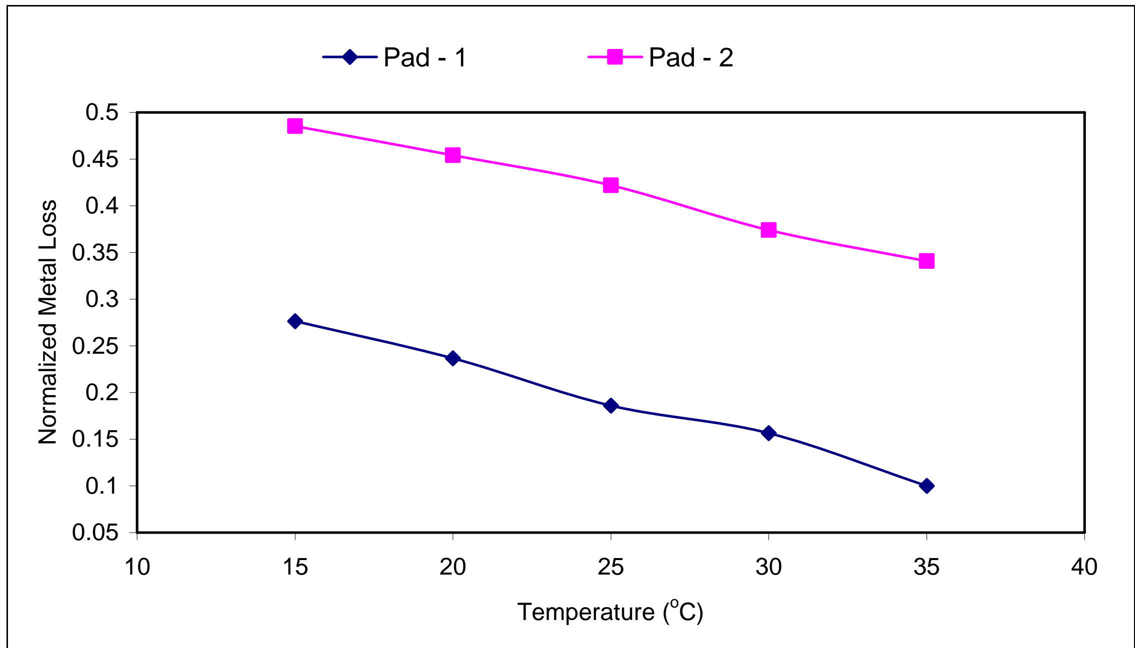

Figure 4.29 Metal Loss vs. Slurry Temperature Using Slurry - 2

From the above observations it can be concluded that the slurry temperature has an effect not only on the surface defects and tribology but also on the change in pad physical and mechanical properties. Further it could be inferred that the surface defects and change in coefficient of friction (COF) is not solely due to the effect of slurry temperature but could be termed due to the interaction factor of slurry temperature and pad properties. Also it can be observed that the slurry type and the chemical constituents of the slurry along with temperature plays a major role in defect generation.

4.6 Analysis of Adhesion Failure and Mechanical Properties with Slurry Temperature

The copper films on some samples got peeled off during polishing with increase in temperature. Figure 4.30 shows the copper films after polishing at various temperatures. The films remained undamaged at temperatures in the range of 15-20 ºC and then started to peel with rise in temperature. The most damaged films were at 35 ºC.

Figure 4.30 Pictures Showing Peeling on Wafers Polished at Different Temperatures. A) Wafer Polished at 15 ºC. B) Wafer Polished at 20 ºC. C) Wafer Polished at 25 ºC. D) Wafer Polished at 30 ºC. E) Wafer Polished at 35 ºC

This might be due to the reason that the wafers have a low-k material beneath the copper, which have low adhesion and mechanical strength causing copper to peel off. This proves that the material (low-k) properties degrade with increase in polishing temperature.

Further in order to investigate the structural changes if any with increase in polishing temperature using X-ray diffraction (XRD) analysis a series of experiments were conducted. These experiments were performed at three different temperatures (15, 25 and 30 ºC) using pad A and different copper polishing slurry. The wafers used were 2 inch blanket copper wafers having 10000 Aº thick copper films. The wafers were polished for different times depending on the temperature at which they were being polished so that same amount of copper is removed from all the wafers. The removal rate and time was calculated using the coefficient of friction graphs as in first and second

series of experiments. Figure 4.31 shows the XRD graph of the wafers polished at different temperatures and also on an as-is copper blanket wafer.

The XRD spectra as collected were compared on unpolished (as-is) and polished samples. It can be seen from Fig. 4.31 that all the films exhibit X-ray reflection from Cu (111), (200), (220), and (222) planes. For all the films, strongest x-ray reflections are visible from Cu (111) planes. The intensity of reflections from Cu (220) is second highest. This indicates that crystallization occurs preferentially in (111) and (220) directions. In order to investigate the evolution of crystallite orientations due to polishing at different temperatures the peak intensities can be compared. It can be seen from the figure that that the evolution of peaks in all the orientations increases with the increase in slurry temperature. The evolution is so prominent with temperature that the peak in (2 1 1) direction does not even exist in the sample polished at 15 ºC slurry temperature.

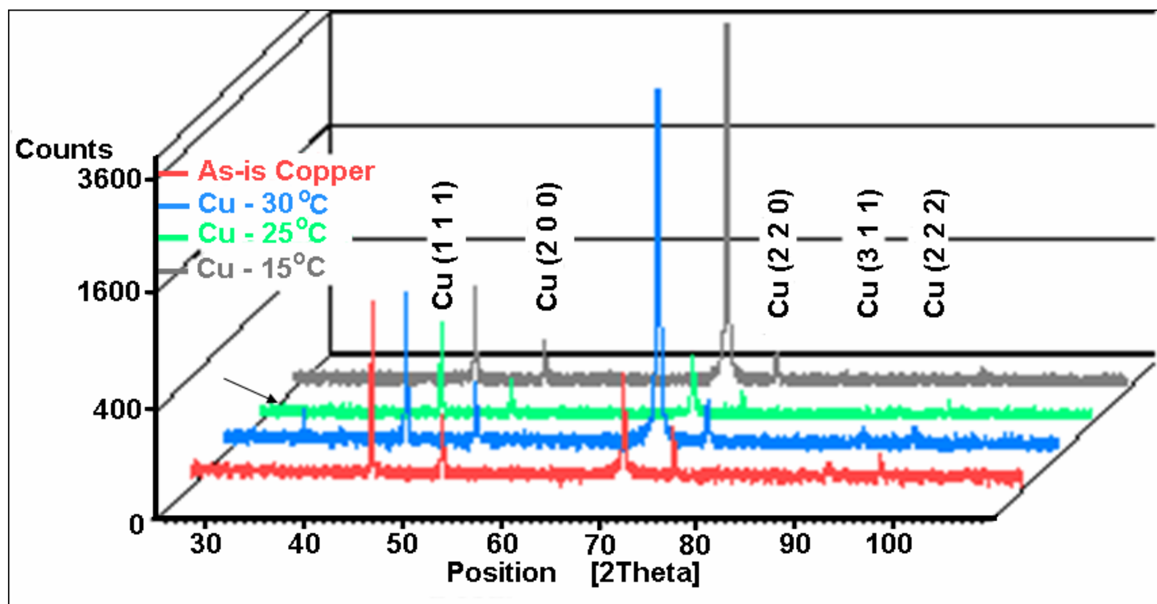

Figure 4.31 Graphs Showing XRD Peaks on Copper Wafers Polished at Different Temperatures

Also from the XRD measurements as shown in figure 4.31, an additional peak at 32 deg diffraction angle was observed on the sample polished at 30 ^{o}C temperature. This indicates that the copper crystallinity increases with increasing polishing temperature. As the crystallinity increases, the mechanical characteristics improve as well and this was confirmed with the hardness tests conducted on the samples using a nano-indenter.

Figure 4.32 presents the hardness of the unpolished film and for the films post CMP at different temperatures. From figure 4.32 it can be noted that the hardness of the polished copper surface increased with increasing slurry temperature. The unpolished sample had significantly lower hardness than the polished ones. This change can be attributed to the work hardening phenomenon during CMP. The work hardening phenomenon appears to be more influential at elevated temperatures. Similarly the modulus of the polished and unpolished thin films along the penetration depth is presented in figure 4.33. It can be seen that the modulus of elasticity increases with increasing slurry temperature. Also, the modulus of elasticity of the unpolished film is significantly lower than that of the polished samples. The numerical data from the nanoindentation experiments is presented in table 4.5 which presents in detail the change in mechanical properties of thin films with a change in slurry temperature.

Table 4.5 Mechanical Properties of Copper Thin Films Before and After Polishing

Sample	Modulus (Gpa)	Hardness (Gpa)
Unpolished Cu	118.51 ± 3.72	1.22 ± 0.06
Polished at 15 C	136.38 ± 5.45	1.57 ± 0.087
Polished at 25 C	136.29 ± 4.77	1.66 ± 0.093
Polished at 30 C	143.45 ± 2.98	1.72 ± 0.068

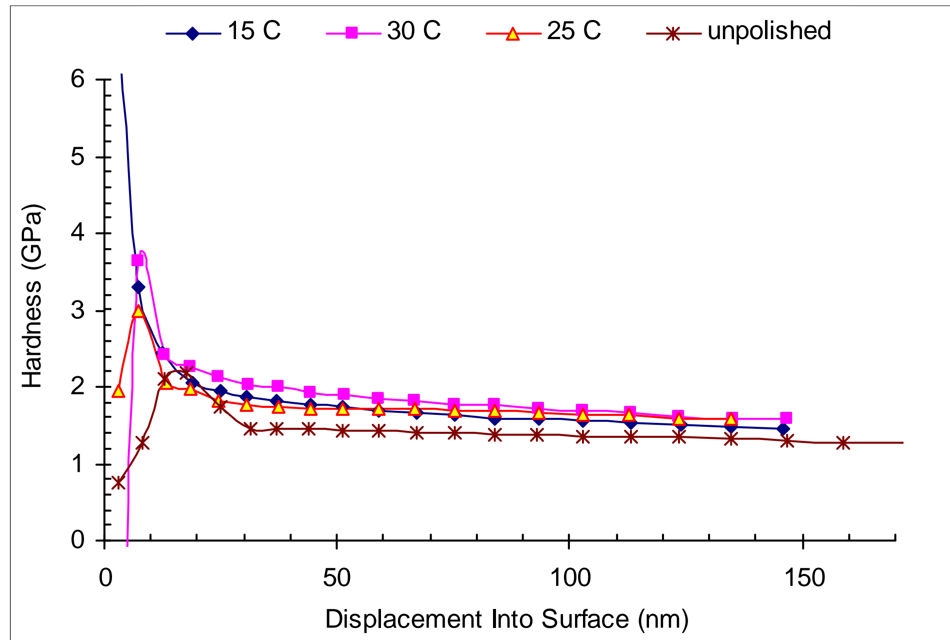

Figure 4.32 Hardness vs. Displacement into Surface for Unpolished and Polished Copper Samples

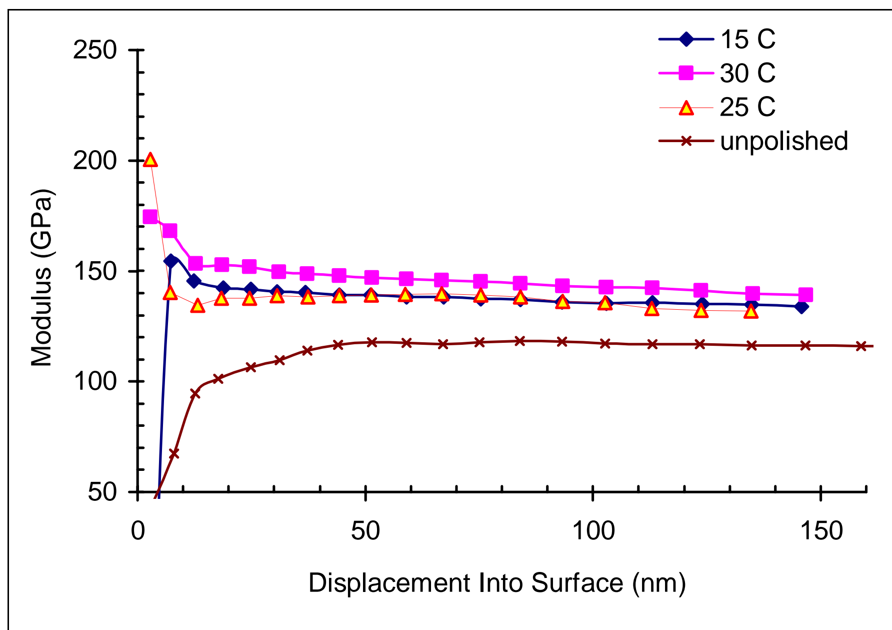

Figure 4.33 Modulus vs. Displacement into Surface for Polished and Unpolished Copper Samples

4.7 Analysis of Electrical Properties with Slurry Temperature

In order to further investigate the effects of surface defects, due rise in polishing temperature on device operating characteristics the second series of experiments were carried out. These experiments were carried on same types of polishing pads (pad 1 & 2) and with same slurry, other parameters remaining the same. The fabricated PMOS devices had similar feature sizes of 10, 20 & 50 μm and bond pads of 100 μm in dimensions as in first set of experiments.

The dishing values and metal loss values were almost numerically similar to the values obtained in the first set of experiments. Then the polished samples were tested for the I-V characteristics using HP 4145B parameter analyzer. Figures 4.34, 4.35 show the transfer curves and sub threshold log plots I-V characteristics of the devices polished at different temperatures.

For the drain characteristics the drain to source voltage (V_{DS}) was swept from 0 to -15 V and the gate to source voltage (V_{GS}) was increased in steps from 0 to -15 V and the corresponding values of drain current (I_D) were recorded. In order to explain the shape of drain characteristics the curve may be divided into four regions as shown in figure 13a. The first region in the curve shown as 0A is the ohmic region. In this region the drain current increases linearly with increase in drain voltage, obeying Ohm's law. In the next region (AB) the drain current increases according to the reverse square law. Here the drain current increases slowly as compared to the ohmic region. This occurs due to the fact that with increase in V_D, the I_D increases. As a result of this, the size of the depletion region becomes bigger, reducing the effective width of the channel. The region under the curve BC is the saturation or the constant current region. Here the drain current reaches

its maximum value and does not increase further even with increase in drain voltage. The region beyond this is known as the breakdown region, in the region the drain current increases rapidly as the drain voltage is increased leading to breakdown of the device.

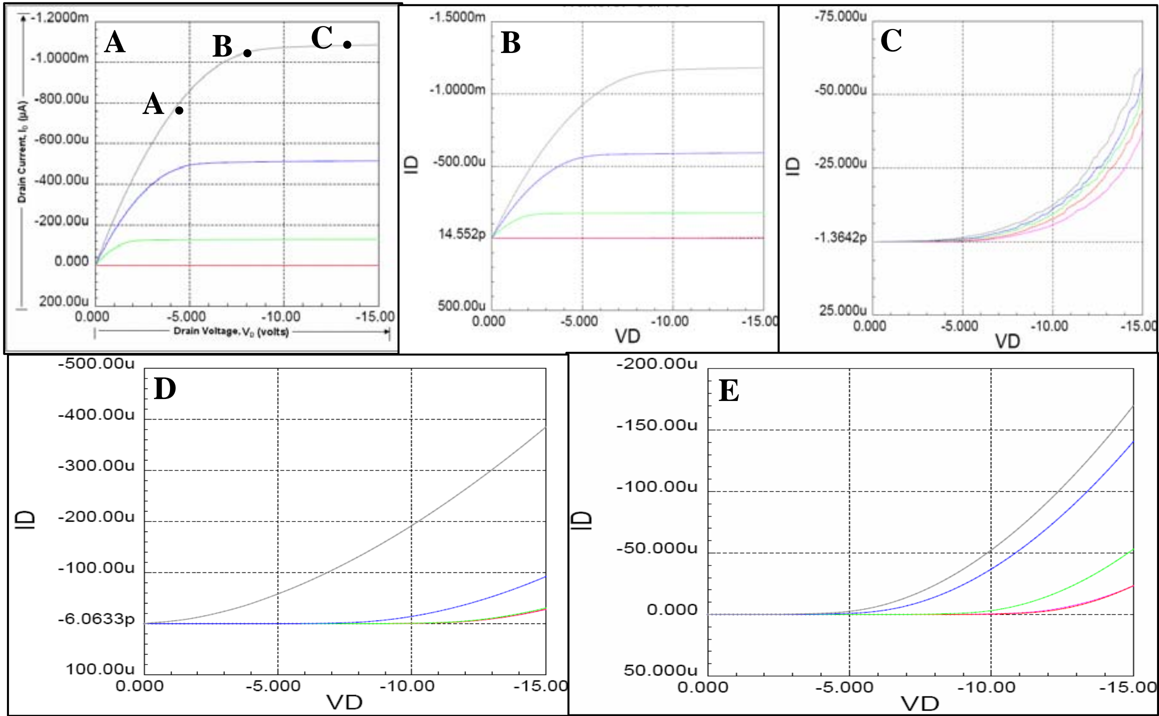

Figure 4.34 Graphs Showing Transfer Curves (I-V Characteristics) of Wafers Polished at Different Temperatures. A) Wafer Polished at 15 ºC. B) Wafer Polished at 20 ºC. C) Wafer Polished at 25 ºC. D) Wafer Polished at 30 ºC. E) Wafer Polished at 35 ºC

It has already been observed that with increase in temperature the amount of surface defects i.e., dishing and metal loss also increase. From figure 4.34 it can be seen that wafers polished at temperatures 15 and 20 ºC operated well in accordance with the operating characteristics, further on wafers polished at higher temperatures 25 and 35 ºC the devices either reached the breakdown region at very low values of drain current or did not operate in the ohmic region, which are not the desired operating characteristics. Whereas on the wafer polished at 30 ºC, the wafer with highest amount of dishing values, the device failed to operate completely (see fig. 4.34).

The transfer curve also called as transconductance curves gives the relationship between drain current and gate voltage. For the sub threshold (transfer) characteristics the gate to source voltage (V_{GS}) was swept from 0 to -25 V and the corresponding values of current (I_D) were recorded. In order to explain the shape of drain characteristics the curve may be divided into three regions as shown in figure 14a. The first region is known as the threshold region. A minimum gate voltage is required in practical to produce a inversion layer, known as the gate threshold voltage ($V_{G(th)}$). In a ideal situation when the gate voltage is less than the threshold voltage no current flows from drain to source, but in practical a very less amount of current flows from drain to source. When the gate voltage is greater than threshold voltage, the inversion layer connects the drain and source and we get significant value of current. From figure 4.35 it could be seen that at wafers polished at lower temperatures 15 and 20 ºC the device the threshold voltage was around 3 volts, further on wafer polished at higher temperatures 25 and 35 ºC the threshold voltage was in between 14-16 volts. Whereas on the wafer polished at 30 ºC, the wafer with highest amount of dishing values, the device failed to operate completely (see fig. 4.35). After crossing the threshold voltage the current increases sharply and then reaches the saturation point and then reaches the breakdown voltage. From these results it can be said that the increase in temperature increases the surface defects which in turn results in device failure.

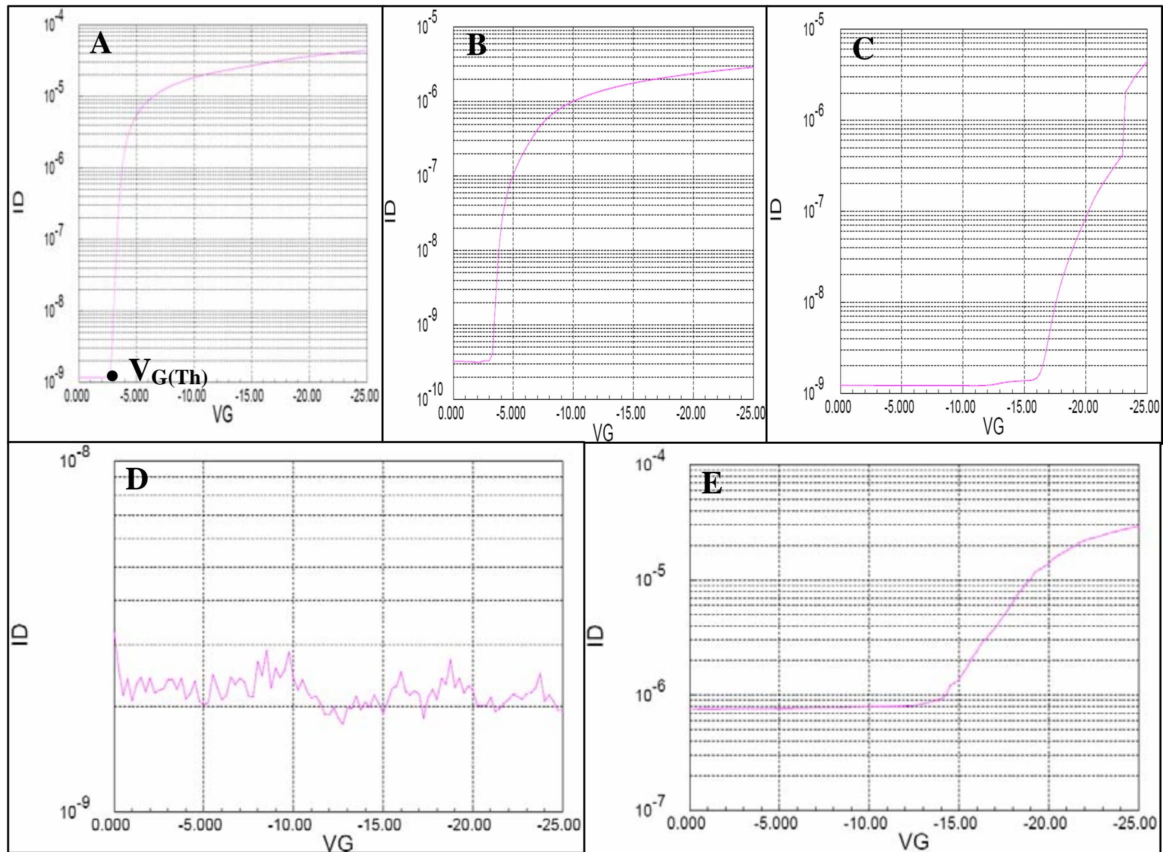

Figure 4.35 Graphs Showing Sub-Threshold Log Plot Curves (I-V Characteristics) of Wafers Polished at Different Temperatures. A) Wafer Polished at 15 ºC. B) Wafer Polished at 20 ºC. C) Wafer Polished at 25 ºC. D) Wafer Polished at 30 ºC. E) Wafer Polished at 35 ºC

From figures 4.34 and 4.35 it could be interpreted that at wafers polished at lower temperatures (15 and 20 ºC) the device operated normally, further on wafer polished at higher temperatures (25 and 35 ºC) the device properties degraded (see fig. 4.34 & 4.35). Whereas on the wafer polished at 30 ºC, the wafer with highest amount of dishing values, the device failed to operate completely (see fig. 4.34). From these results it can be said that the increase in temperature increases the surface defects which in turn results in device failure.

4.8 Summary

The effect of slurry temperature at three temperatures on two different pads were investigated, keeping the pressure and platen velocity constant. The patterned copper samples were characterized using the AFM and profilometer. The characteristics of two different kinds of pads were analyzed using DMA. From the DMA analysis it could be inferred that pad softens with increase in temperature and pad B is softer in nature compared to pad A. Within the operating range there is greater percentage of decrease in storage modulus of pad B compared to pad A. From SEM analysis it was found that pad conditioning improved the uniformity of polish and also increased the roughness of the polishing pad. It was found that the COF on pad A increased with increase in slurry temperature and on pad B the variation in COF with increase in slurry temperature was found to be statistically insignificant. This change in COF on the pads can be attributed to the pad physical properties. The removal rates on both the pads increased with increase in slurry temperature. However the removal rate on pad A was higher than the removal rates on pad B. This increase in removal rate and the difference in the amount of removal rates on both pads can be attributed to the change in the rate of kinetics of chemical reactions and also to the mechanical properties of the pad.

The dishing initially increased with increase in temperature upto 30 ^{o}C and then decreased with further increase in temperature using slurry 1, whereas the dishing decreased with increase in slurry temperature using slurry 2. This could be attributed to the change in the properties of surface asperities of the pad. This could be well explained with the DMA analysis of pad materials. It further concluded that the dishing was dependent on the interaction factor of slurry temperature, slurry type (chemical

constituents of the slurry) and change in pad properties with temperature, than as initially thought would be due to slurry temperature. Also changes in copper structural properties were observed with increase in slurry temperature. The device electrical properties degraded drastically with increasing slurry temperature and even leading to device failure at higher polishing temperatures.

Chapter 5

Conclusions and Future Work

The main objective of this research was to study the effect of slurry temperature on defect generation and tribology during copper CMP. Surface defect generation on patterned copper wafers with increase in slurry temperatures were tested using the CMP tester at different temperatures and with two types of polishing pads. Post CMP analysis of the polished samples was conducted using atomic force microscopy (AFM) and profilometer. The mechanical and physical properties of the polishing pads used were analyzed using dynamic mechanical analysis (DMA). Change in copper structural properties was studied using X-ray diffraction (XRD) analysis. Also the device electrical working characteristics were used on fabricated devices polished at different slurry temperatures. Conclusions based on the research work and the results from previous chapters are presented here.

5.1 Conclusions

5.1.1 Friction (COF) and Removal Rate Studies

- The coefficient of friction (COF) on pad A and pad B increased with the increase in slurry temperature.
- This increase in coefficient of friction on pad A and pad B can be attributed to increased area of contact of pad-wafer surface with increase in slurry temperature, resulting in higher shear force at the interface.

- The removal rate increased with increase in slurry temperature on both pad A and pad B.
- With increase in slurry temperature the removal rate on pad A was higher compared to pad B depending on the interconnect line width.
- This variation in removal rates on two polishing pads can be attributed to pad hardness and other pad mechanical properties. Also this variation can be attributed to change in the rate of kinetics of chemical reactions with increase in slurry temperature.

5.1.2 Dishing and Metal Loss

- The dishing and metal loss initially increased with increase in temperature from 15 °C to 30 °C and then decreased with further increase in temperature on both pads with slurry-1.
- This phenomenon of increase in dishing and metal loss initially and then decrease can be attributed to local softening of pad and change in pad physical and mechanical properties.
- The dishing decreased with increase in slurry temperature using slurry-2. This phenomenon can be attributed to the chemical nature (oxidizer and other constituents of the slurry) of the slurry and its interaction with pad and also change in its chemical properties with temperature rise.
- The different trend in dishing pattern with two different types of slurries is due to change in pH of slurry with increase in temperature.

- The amount of dishing on 10 µm metal line was higher on pad B compared to pad A, but whereas with increase in the line width the dishing with pad A is higher than dishing on pad B.
- This variation in dishing with different types of pads can be attributed to change in the properties of surface asperities of the pad and also change in chemical dissolution rate.
- The DMA analysis confirms that with increase in temperature the pad becomes softer.
- The amount of decrease in percentage of storage modulus of pad material is higher for pad B compared to pad A. But in an ideal case there should be no change in storage modulus for a polishing pad within the operating temperature range.
- Pad B has lower glass transition temperature (Tg) compared to pad A. After reaching Tg the pad transform from a glassy state into a rubbery state.
- Due to the softening of the pad with the increase in temperature the pad asperities reach deeper into the metal lines and cause dishing and metal loss.
- Dishing and metal loss were dependent on the interaction factor of slurry temperature and change in pad properties rather than only with the slurry temperature.
- Also the uniformity in polishing improved with pad conditioning. The conditioning also improved the roughness of the polishing pad.

5.1.3 Film Mechanical and Electrical Properties

- The films peeled off at higher temperatures. At 35 ºC the copper films on some of the samples completely peeled off due to adhesion problems.
- The structural properties improved with increase in slurry temperature. There was an increase in crystallinity of the copper thin films and also hardness and modulus increased with increase in polishing temperature.
- An extra peak at (2 1 1) was observed on the film polished at 30 ºC indicating a change in crystallinity.
- The electrical properties degraded drastically with increase in slurry temperature. At the highest temperature the devices even failed to operate.
- The devices with minimal or mo dishing operated perfectly and exhibited good I-V characteristics. The devices/wafers polished at 35 ºC failed to operate completely.

5.2 Future Work

The effect of interaction of other process conditions such as pressure and velocity with slurry temperature can be investigated. Also the effect of slurry temperature on surface defects and tribology can be studied using various acidic and basic slurries and also with various types of oxidizers and concentration of oxidizers. The effect of various particles sizes, particle concentrations and different kinds of abrasive particles can be studied. The effect of various orientations on pad surfaces such as grooves and perforations along with different kinds of pad materials can be investigated. Also various methods to reduce the temperature during polishing can be studied in order to reduce the

surface defects. The electrochemical analysis on different slurries can be done to get a better understanding of change in slurry characteristics with change in temperature.

References

1. Joseph M. Steigerwald, Shyam P. Murarka, Ronald J. Gutmann, Chemical Mechanical Planarization of Microelectronic Materials, John Wiley and Sons, Inc. New York, (1997).

2. J.G. Ryan, R.M. Geffken, N.R. Poulin, J.R. Paraszczak, The Evolution of Interconnection Technology at IBM, IBM J. Res. Dev., 39, 371, (1995).

3. S. Wolf, Silicon Processing For the VLSI Era, Vol. 4, Lattice Press, California, (2002).

4. Internet Website: http://www.itrs.net/Links/2005ITRS/Home2005.htm, ITRS, (2005).

5. V. R. Kakireddy, R. Mudhivarthi, A. Kumar, P. Lefevre, Proc. VLSI Multilevel Interconnect Conference, 050, 415-420 (2006).

6. J. M. Steigerwald, S. P. Murarka, R. J. Gutmann, D. J. Duquette, Materials Chemistry and Physics, 41, 217-228, (1995).

7. R. Carpio, J. Farkas, R. Jairath, Thin Solid Films, 266, 238-244, (1995).

8. Y. S. Obeng, J. E. Ramsdell, S. Deshpande, S. C. Kuiry, K. Chamma, K. A. Richardson, and S. Seal, IEEE Transactions on Semiconductor Manufacturing, 18, 4, (2005).

9. A. Ishikawa, H. Matsuo, T. Kikkawa, J.Electrochem. Soc. 152, (9), G695-G697, (2005).

10. Z. Li, K. Ina, P. Lefevre, I. Koshiyama, A. Philipossian, J.Electrochem. Soc. 152, (4), G299-G304, (2005).

11. Y. Nomura, H. Ono, H. Terazaki, Y. Kamigata, M. Yoshida, Materials Research Society Symp. Proc., 816, (2004).

12. Z. Li, P. Lefevre, I. Koshiyama, K. Ina, D. Boning, and A. Philipossian, IEEE Transactions on Semiconductor Manufacturing, 18, 4, (2005).

13. H. Lu, B. Fookes, Y. Obeng, S. Machinski, K.A. Richardson, Materials Characterization, 49, 35-44, (2002).

14. H. Lu, Y. Obeng, K.A. Richardson, Materials Characterization, 49, 177-186, (2003).

15. L. Wang, and F. M. Doyle, Proc. CMP Multilevel Interconnections Conference, (2004).

16. J. Sorooshian, D. DeNardis, L. Charns, Z. Li, F. Shadman, D. Boning, D. Hetherington, and A. Philipossian, J. Electrochem. Soc., 151(2), G85-G88, (2004).

17. P. A. Miranda, J. A. Imonigie, A. L. Erbe, A. J. Moll, IEEE WMED, (2005).

18. T. H. Tsai, Y. F. Wu, S. C. Yen, Applied Surface Science, Article in press, (2003).

19. P. A. Miranda, J. A. Imonigie, and A. J. Moll, J. Electrochem. Soc., 153(3), G211-G217, (2006).

20. P. Leduc, M. Savoye, S. Maitrejean, D. Scevola, V. Jousseaume, G. Passemard, IEEE, (2005).

21. Q. Luo, D. R. Campbell, S. V. Babu, Thin Solid Films, 311, 177-182, (1997).

22. A. E. Miller, P. B. Fischer, A. D. Feller, K. C. Cadien, IEEE, 143-145, (2001).

23. T. Du, D. Tamboli, V. Desai, Microelectronic Engineering, 1, (2003).

24. S. Mudhivarthi, N. Gitis, S. Kuiry, M. Vinogradov, and A. Kumar, J.Electrochem. Soc. 153, (5), G372-G378, (2006).

25. S. Mudhviarthi et al, Electrochem. Solid-State Lett., 8, (9), G241-G245, (2005).

26. L. Borucki, Z. Li, and A. Philipossian, J. Electrochem. Soc., 151, G559 (2004)

27. Len Borucki, Leslie Charns and Ara Philipossian, J. Electrochem. Soc., 151, (12), (2004), G809-G813.

28. Z. Li, L. Borucki, I. Koshiyama, and A. Philipossian, J. Electrochem. Soc., 151, (7), G482-G487, (2004).

29. V. R. K. Gorantla, K. A. Assiongbon, S. V. Babu, and D. Roy, J. Electrochem. Soc., 152, (5), G404-G410, (2005).

30. V. R. K. Gorantla, A. Babel, S. Pandija, and S. V. Babu, Electrochem. Solid-State Lett., 8, (5), G131-G134, (2005).

31. J. M. Steigerwald, R. Zirpoli, S. P. Murarka, D. Price, and R. J. Gutmann, J. Electrochem. Soc., 141, 2842, (1994).

32. F. Preston, J. Soc. Glass Tech., 11, 214, (1927).

33. Internet Website: www.wikipedia.org.

34. S. Wolf, and R. N. Tauber, Silicon Processing For the VLSI Era, Vol. 1, Lattice Press, California, (2000).

35. Internet Website: www.pubs.acs.org, American Chemical Society.

36. J. D. Reid, "Fundamentals of Copper Electroplating," Semiconductor International, June 1998, p. 94.

37. Internet Website: www.mems-exchange.org.

38. V. M. Dubin et al, Proc. VLSI Multilevel Interconnect Conference, p. 315, (1995).

39. P. B. Zantye, A. Kumar and A.K. Sikder "Chemical mechanical planarization for microelectronics applications", Materials Science and Engineering: R: Reports, 45 (3-6) pp. 89 (2004).

40. H. H. Uhlig, Corrosion and Corrosion Control, John Wiley and Sons Inc., New York, (1985).

41. M. R. Oliver, Chemical Mechanical Planarization of Semiconductor Materials, Springer Series in Materials Science, New York, (2004).

42. Internet Website: http://nnrc.eng.usf.edu, University of South Florida.

43. Internet Website: http://acept.la.asu.edu/PiN/rdg/elmicr/elmicr.shtml, Arizona State University.

44. I. Li, K. M. Forsthoefel, K. A. Richardson, Y. S. Obeng, W. G. Easter, and A. Maury, Mat. Res. Soc. Symp., 613, (2000).

45. Kevin P. Menard, Dynamic Mechanical Analysis, CRC Press Inc., Florida, (1999).

46. A. Tregub, M. Moinpur, and J. Sorooshian, "Effect of Temperature on Thermoanalytical Properties of Polishing Pads."

47. J. Luo, D. A. Dornfeld, IEEE Transactions on Semiconductor Manufacturing, 14 (2), 112-133, 2001.

48. Internet Website: http://uweb.cas.usf.edu/~harmon, University of South Florida.

49. P. Singer, "Copper CMP: Taking aim at dishing," Semiconductor International, October 2004.

50. G. Fu and A. Chandra, J. Electronic Materials, 31 (10), 1066-1073, 2002.

51. Internet Website: http://pubs.usgs.gov/of/2001/of01-041/htmldocs/images/xrdschem.jpg.

52. N. Gitis, *Semiconductor Fabtech*, 18, 125 (2003).

53. N. Gitis, U.S. Pat. 6,494,765 (2002).

54. N. Gitis, U.S. Pat. 6,702,646 (2004).

55. N. Gitis and M. Vinogradov, in *Proceedings of 2nd ICMI*, Santa Clara, CA (2001).

56. A. Sikder, A. Kumar *J. Electron. Mater.*, 30, 1520 (2001).